UNIVERSITY OF CAPE TOWN
IYUNIVESITHI YASEKAPA • UNIVERSITEIT VAN KAAPSTAD

Machine design to improve accuracy and repeatability in on-site circular milling

---

Author:
Jethro Berry

Supervised by:
Associate Professor Franz-Josef Kahlen

A dissertation submitted to the Department of Mechanical Engineering, University of Cape Town, in full fulfilment of the requirements for the degree of Masters of Science in Engineering.

Cape Town, South Africa

31 August 2010

Plagiarism Declaration

I know the meaning of plagiarism and declare that all the work in the document, save for that which is properly acknowledged, is my own.

Abstract

This project's objective focuses on machine design to primarily improve accuracy and repeatability in on-site circular machining. On-site circular machining is used in the finishing and repairing of flanges most commonly used for mating with slewing bearings. The expected outcomes of the manufacturing processes are always increasing, therefore requiring higher levels of accuracy. The milling must be performed under a wide range of environmental conditions. Temperatures ranging from -17°C at the top of a wind turbine tower to +40°C inside a steel mill have been experienced. The environmental conditions may prohibit the use of high accuracy measurement systems. The factors that effect the achievable accuracy and repeatability of the circular milling process are assessed in this project. The potential for a limit to the achievable accuracy is also assessed later in the text. From these findings new systems are designed in order to achieve higher degrees of performance in the circular milling process over a larger range of operating conditions.

Acknowledgments

I would like to thank the following people:

- I would like to thank Stefan Wagner, the managing director of Wagner GmbH for his continuous support and advice within project.
- My fiancée Claire for all the help and support she has given me over the duration of this project.
- My Parents for all their support and encouragement in life and my studies.
- Associate Professor Kahlen who has supervised and guided me through the process of this project.
- The staff of Wagner GmbH, namely Dorothee Daun and Stefan Schmitz.
- The machinists who took the time to ensure that the highest quality was achieved with each component.

Table of Contents

Plagiarism Declaration i

Abstract ii

Acknowledgments iii

Table of Contents iv

List of Figures vii

List of Tables x

1. Introduction 1

1.1. On-Site Machining Background 1

1.2. Project Overview 4

1.3. Circular Milling 5

2. Literature Review 7

2.1. Main Subassemblies 7

2.2. Machine Coordinate System 9

2.3. Reference Planes 9

2.4. Wagner GmbH 10

2.5. The M151 and M259 Circular Milling Machines 11

2.6. The M391 Circular Milling Machine 13

2.7. Industrial Circular Mills 14

2.8. Current Design Features 16

2.9. Flange Deformation and Un-Flatness 19

2.10. Cutting Forces 22

3. Metrology 24

3.1. Methods of Measuring Machined Surface Quality. 24
3.2. Current Measurement and Alignment Protocols 28
3.3. Protocol 1 29
3.4. Protocol 2 30
3.5. Downfalls of Existing Protocols 31
3.6. False Method 32
3.7. Deflection Simulation 33
3.8. Current Evaluation 36
4. Methodology 38
4.1. Aim 38
4.2. Test Conditions 38
4.3. Milling Tests 41
4.4. Results of Milling Tests 43
4.5. Discussion of Milling Test Results 46
4.6. Comments on Existing Designs 50
5. Design 52
5.1. Design Specifications 52
5.2. Leg Interface and Internal Reference Plane 53
5.3. Cassette 59
5.4. Arms 63
6. Validation 77
6.1. Internal Referencing System Validation 78
6.2. M391 Achievable Un-Flatness 82
7. Conclusions 83

8. References 86
Appendix A: Milling Test Results 88
Appendix B: Results of 5.4.5. Simulation 2 93
Appendix C: M391 Validation Results 95
Appendix D: Drawings 97

List of Figures

Figure 1: On-Site milling of the base of a metal shredder set in concrete foundations. 1

Figure 2: A traditional lathe (left) and portable lathe (right). 3

Figure 3: Basic anatomy of wind turbines. Image courtesy of Rothe Erde GmbH [2]. 5

Figure 4: A circular milling machine operating on an installed wind tower. 6

Figure 5: Circular mill operating vertically when mounted to an unassembled wind tower section. 7

Figure 6: Machine Coordinate system. 9

Figure 7: Machine cutting plane. 9

Figure 8: Grinding the mating surfaces for a slewing bearing, 1993. 10

Figure 9: M151 circular mill vertically mounted to a wind tower. 11

Figure 10: M259 milling a surface in a hydro electric power station. 12

Figure 11: SILK AX48-120 flange facer [3]. 14

Figure 12: Climax CM6000 [4]. 15

Figure 13: SLM Circular self levelling machine [5]. 16

Figure 14: Base of M151 with arm removed. 17

Figure 15: M151 foot. 18

Figure 16: M259 foot. 18

Figure 17: Two planes representing the total un-flatness of a flange. 19

Figure 18: Illustration of taper error of a flange. 19

Figure 19: Forces acting on work relative to tool insert and cutting geometry. 22

Figure 20: Resultant cutting forces on work relative to milling machine. 23

Figure 21: The major components of a typical surface texture [12]. 25

Figure 22: Representation of the digital levelling process. 26
Figure 23: Dial gauge measuring flatness of a gear mounted to a milling machine. 27
Figure 24: Top view of the mounting positions of the feet with the M151 and M259. 29
Figure 25: Illustration of protocol 2. 30
Figure 27: Orientation relative to axis. 31
Figure 26: Orientation relative to flange (side view). 31
Figure 28: False alignment of the cutting plane with the existing surface. 32
Figure 29: Deflection simulation model. 33
Figure 30: Deflection of slewing bearing under poor setup conditions. 34
Figure 31: Slewing bearing support structure. 35
Figure 32: Inverted milling of a harbour crane upper bearing seating. 36
Figure 33: Dial gauge measuring between the milling head and surface. 37
Figure 34: M151 during testing phase. 39
Figure 35: Magnetic base, pivoting joint and staff used for measurements. 40
Figure 36: Comparison between the supported and non supported feet. 41
Figure 37: M151 milled surface from Test 2. 42
Figure 38: M151 setup profile with three legs secured. 43
Figure 39: M259 setup profile with three legs secured. 43
Figure 40: Test 1; M151 44
Figure 41: Test 1; M259 44
Figure 42: Test 2; M151 45
Figure 43: Test 2; M259 45
Figure 44: Illustration of offset tool. 47
Figure 45: Measurements of the M151 effected by vibrations. 50

Figure 46: Alignment system and bearing. 55
Figure 47: Separated base leg, leg and foot. 56
Figure 48: Bottom base with emphasised referencing surfaces. 57
Figure 49: M391 foot. 58
Figure 50: M391 and M151 milling head assemblies. 59
Figure 51: Cassette entailing pitch features. 60
Figure 52: Anisotropic lay due do misaligned tool. 61
Figure 53: Cassette and milling head coupling interface. 62
Figure 54: Components of simulation 1c. 65
Figure 55: Axial deflection of horizontal gravity simulation. 74
Figure 56: Circumferential deflection of vertical gravity simulation. 74
Figure 57: Axial deflection in force simulation. 75
Figure 58: Circumferential deflection in force simulation. 75
Figure 59: Comparison of section masses. 76
Figure 60: M391 circular milling machine. 77
Figure 61: M391 setup with 4 legs secured. 79
Figure 62: Dial gauge being used in with the internal reference. 79
Figure 63: M391 setup with 8 legs secured using internal reference plane. 80
Figure 64: M391 Foot. 81
Figure 65: M391 test for limit to un-flatness. 82

List of Tables

Table 1: Physical attributes M151. 12

Table 2: Physical attributes M259. 12

Table 3: Operating diameters for the Wagner GmbH circular mills. 13

Table 4: Rothe Erde un-flatness values [8]. 20

Table 5: Global Bearing Services stiffness tolerances [7]. 20

Table 6: M151 testing conditions. 40

Table 7: M259 testing conditions. 40

Table 8: Simulation 1 results. 65

Table 9: Cutting data. 68

Table 10: Constants for calculating Fc. 68

Table 11: Values for first shear calculation. 69

Table 12: Values from actual shear calculation. 70

Table 13: Forces resolved to machine coordinate system. 71

Table 14: In tolerance test results M151, Figure 40. 88

Table 15: In tolerance test results M259, Figure 41. 89

Table 16: Un-flatness limit and three leg setup test results M151, Figure 38 and Figure 42. 90

Table 17: Un-flatness limit and 3 leg setup test results M259, Figure 39 and Figure 43. 91

Table 18: Vibration influence, Figure 45. 92

Table 19: Results of Section 5.4.5 – simulation 2. 94

Table 20: Internal reference system validation results, Figure 61 and Figure 63. 95

Table 21: Un-flatness test results M391, Figure 65. 96

1. Introduction

1.1. On-Site Machining Background

When a machine operating in industry experiences unforeseen downtime, this inevitably becomes costly to the company involved. It is therefore necessary to perform repairs within as short a time as possible.

Sometimes the component requiring work is constructed on-site and is immobile, preventing it from being transported to a machine shop; or if the component is secured to the enclosure or superstructure on which the machine is mounted. If the said component is part of a large complex assembly that is damaged, it is often not logistically or financially viable to dismantle the entire machine to remove the part. Figure 1 illustrates an example of milling being performed on the casing of a metal shredder in a recycling plant. This casing was set in concrete and it was not possible for the work to be removed and relocated.

Figure 1: On-Site milling of the base of a metal shredder set in concrete foundations.

When a company encounters such problems, on-site machining becomes the only viable option as with on-site machining the machine tool is transported to the work and assembled for machining on-site. On-site machining is also used in the finishing of large assemblies that are constructed on-site as well as the finishing and reconditioning of components that are found to be out of specification on-site.

With on-site machining, regular in-house activities such as milling, turning, drilling, tapping, honing, boring and grinding are carried out at the site of installation. These processes require specialised equipment to be constructed that are adapted for transportability while retaining the ability to meet customer specifications for accuracy and precision.

There are two main challenges that are met in on-site machining:

- the need to repair or refurbish defective components or parts on-site, and
- the need to design machines that are mobile and able to be mounted to the work.

Traditional in-house machines are constructed so as to be mounted to secured foundations and in controlled environments. This type of construction inevitably leads to voluminous and heavy machines that are not easily transportable and unsuitable for on-site machining. In contrast, the on-site machine is constructed to be lightweight and easily transportable.

On-site machines can be categorised into two general groups:

- firstly those that mount directly to the work piece and use integrated prime movers for any movement needed, and
- secondly, those that are mounted to the environment and use the movement of the work piece as the prime mover.

With both groups, the same principles of machining are used as with traditional in-house activities. Often the same tools are used, although the differences in the mounting method between the machine tool and work can lead to devices that use significantly different designs, even though the action performed is functionally the same. Figure 2 is an example of the significant difference in construction and appearance of traditional and portable lathes. In contrast to the bulky fixed lathe (left), the portable device from Wagner GmbH (right) is a rotating frame that is secured to the work. The frame consists of two stationary rings, onto which a rotating inner frame is mounted, and the ring and electric prime mover are connected via a chain. The rings house radial oriented set screws that are used for mounting and alignment with the work. The portable lathe shown is configured to turn a diameter of ϕ800mm and at this diameter the complete assembly weighs less than 200kg, a strong contrast to the fixed lathe weighing approximately 3200kg.

Figure 2: A traditional lathe (left) and portable lathe (right).

As illustrated in Figure 2, considerable emphasis is placed on constructing lightweight machine tools for on-site machining. On-site machining firms such as Wagner GmbH in Eschweiler, Germany are contracted worldwide. With the machine tools often needing to be air freighted to their destinations, the cost of airfreight again emphasises the importance of reduced weight. The emphasis on reduced weight has a disadvantage, by reducing the mass of the machine the susceptibility to be influenced or experience vibrations is increased.

The design of an on-site machine must also take into account the need for the machine to be flexible in its application, avoiding once off machines that are redundant after a single job. These machines are designed to work over as large a range of operational parameters as possible. With the design of on-site machines, the outcome accuracy and repeatability is a key design criteria.

1.2. Project Overview

This section introduces the literature review by assessing the state of the art in the industry which later serves as a basis for comparison. Relevant literature is reviewed, as well as a general synopsis pertaining to the anatomy and co-ordinate systems of circular milling machines.

The operating protocols deployed in the field are specifically assessed in the metrology section. The disadvantages and inadequacies of these systems are highlighted to isolate critical functions. This is followed by the methodology section where the current machines are tested to validate the predicted performance in comparison to the attained results.

The findings of the metrology and methodology sections are used as a basis for the design section. Here, the new design functions are combined with existing operating criteria to create the new designs.

In the final validation section, the manufactured designs are validated and the performance thereof is assessed. The report is concluded with an overall assessment of the results and achievements.

1.3. Circular Milling

Due to the formidable growth of the wind energy sector, there has been a significant increase in wind-turbine capacity worldwide. The World Wind Energy Association reported a 31.7% growth rate in the wind sector, as well as noting a continuing trend that the world capacity doubles every three years [1]. In Figure 3 a slewing bearing is used between the nacelle (upper housing of the turbine mechanics) and the tower. The bearing requires that it be mounted to companion structures with mating surfaces having controlled un-flatness and taper error.

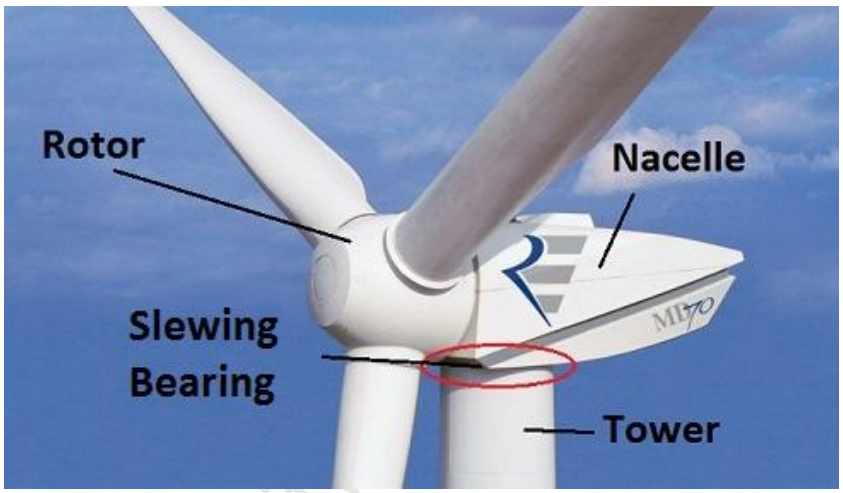

Figure 3: Basic anatomy of wind turbines. Image courtesy of Rothe Erde GmbH [2].

The technology applied in these wind towers is fast progressing to produce larger power outputs, resulting in the overall sizes of the turbines increasing as well as the corresponding forces. This has placed greater emphasis on the performance of the machining processes and tolerances required for the companion structures. These higher requirements provide the opportunity for research and testing to be performed in this field.

This project focuses on repeatability and accuracy in circular face milling of flanges. The findings of the research and testing are incorporated into the design for a newly commissioned circular mill with an aim to improve accuracy and repeatability in the circular milling process.

The circular milling machine is a machine tool that is attached to the work in order to face mill a circular surface. The machine uses a slewing bearing to separate the upper and lower sections of the machine. The lower, stationary section is fixed to the work or environment via adjustable feet that allow for alignment of the machine with the work. The upper, rotating section houses the milling tool assembly which is attached to the rotating base via a segmented arm. When the upper section rotates, this causes the tool to follow a circular, orbital path. Figure 4 illustrates a circular mill installed and operating on an assembled wind tower, operating at a height of 94m.

Figure 4: A circular milling machine operating on an installed wind tower.

The main application of the to be developed machine is the machining of slewing bearing mating surfaces in the wind turbine industry. These slewing bearings are used across a wide range of industries spanning open-pit mining, cranes, swing bridges, tunnelling machines to steel mills. In each application there can be a need for circular milling in repairing or finishing the mating surfaces. The surfaces require that the total un-flatness is machined to within the specification set by the manufacturer. This also prevents localised deformation in the bearing raceway which in turn causes increased stresses and reduced lifespan of the bearing.

2. Literature Review

This section contains supporting information used in this project.

2.1. Main Subassemblies

The following descriptions detail the main subassemblies referred to in this project. For reference, the image in Figure 5 is indexed corresponding to the descriptions found on the following page.

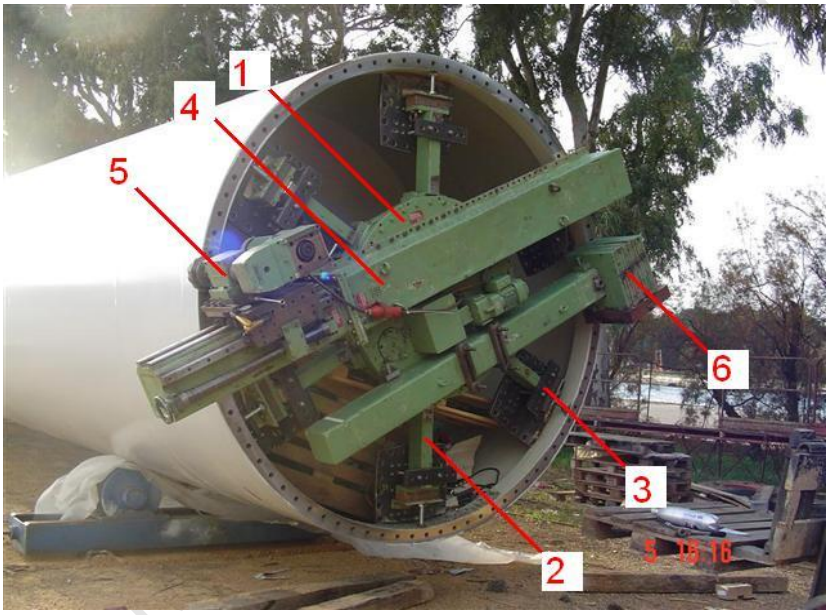

Figure 5: Circular mill operating vertically when mounted to an unassembled wind tower section.

Stationary Subassemblies

1 – Body

The core or chassis of the machine onto which all other subassemblies mount, separating the stationary bottom and rotating top by means of a slewing bearing.

2 – Legs

Used to attain the required mounting diameter for the stationary base. Combinations of leg segments of different lengths can be combined to attain the approximate mounting diameter. The legs are mounted to the stationary, lower section of the body (1).

3 – Feet

The direct interface between the mounting surface and the machine. Its functionality is to allow for final adjustments made to the positioning of the machine. Adjustment in the radial and axial directions allow for the fine adjustments required to attain concentricity and parallelism to the desired plane. The feet are mounted to the end of the legs (2).

Rotating Subassemblies

4 – Arm

Interface between the milling head (5) and the base (1) of the machine. Combinations of arm extenders as well as linear guides mounted in the radial direction are used to attain operating diameters for the tool.

5 – Milling head assembly

Houses the milling head, milling motor and mechanisms for feed in the z direction. The milling head assembly is mounted to the end of the arm (4) assembly.

6 – Counterweight

Mounted directly to the rotating upper section of the body. Counteracts the moment created by the arm and milling head assembly. Used primarily during upright milling activities.

2.2. Machine Coordinate System

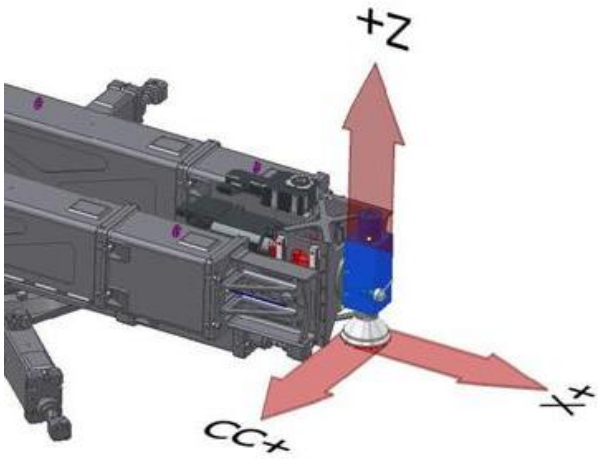

Figure 6: Machine Coordinate system.

Z-axis (axial direction):

Positive: the direction opposite to gravity when the machine is mounted parallel to the horizon.

X-axis (radial direction):

Radial movement of the tool. Outward direction from centre of machine is defined as positive.

CC – cutting circumference:

Rotation of tool about the Z-axis. Clockwise is defined as positive.

The positive directions for each axis are illustrated in Figure 6.

2.3. Reference Planes

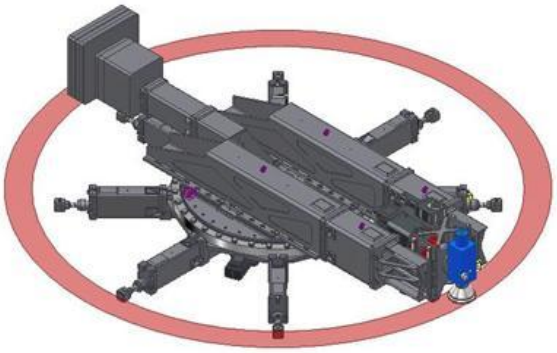

Figure 7: Machine cutting plane.

The cutting plane or machine plane:

The plane defined by tool when the machine completes one full revolution about the z-axis (illustrated in Figure 7).

The reference plane:

The external reference plane defined by the levelling device or similar measurement device.

The desired plane:

The surface orientation defined by the customer.

2.4. Wagner GmbH

Wagner GmbH in Eschweiler, Germany is a refurbishing and manufacturing firm specialising in on-site mechanical services. In 1993 Wagner GmbH was specifically contracted by a client to perform the surfacing of two mating surfaces for a slewing bearing of ϕ4000mm where the clearance between the surfaces was maximum 300mm. At this time the surfacing of such surfaces was performed using on-site flange-turning devices. The restricted clearance, illustrated in Figure 8, prevented the use of the existing lathes, since they were too large to operate in the confined space.

Figure 8: Grinding the mating surfaces for a slewing bearing, 1993.

As an innovation, Wagner GmbH constructed a low height orbital grinding machine. The concept was successful as it permitted machining of a larger surface area per orbit. Although was restricted by small grinding engagements relative to the existing turning capabilities which resulted in longer machining times The machine used a poor quality bearing in the base that was not play free. This too was a source of error. In order to improve the time used, a ϕ80mm face milling head was attached to the grinding machine. This proved to be successful, with a significantly reduced time required over turning and grinding. The grinding process produced a anisotropic surface pattern which was an improvement compared with the isotropic patterns produced in turning.

Subsequently, in 1994 Wagner GmbH commissioned its first circular milling machine. This first machine, namely machine number M151, has, with gained experience, been modified and improved to date. In 1998 a second circular mill, the M259, was commissioned with the main intention of operating at larger diameters. The two machines are discussed below.

2.5. The M151 and M259 Circular Milling Machines

To date, Wagner GmbH utilises two circular milling machines. Both machines were designed and manufactured in house. These machines are built in such a way that they may be transported in regular containers for air freight and then can be assembled on-site. The text that follows details the critical aspects of the two machines. In the text the machines are referred to by their Wagner GmbH machine numbers, M151 (Figure 9) and M259 (Figure 10) respectively.

M151

Figure 9: M151 circular mill vertically mounted to a wind tower.

Construction year	1992
Approximate weight	2800kg (at max diameter)
Minimum working diameter	2000mm
Maximum working diameter	5000mm
Minimum height	1050mm
Number of legs	6

Table 1: Physical attributes M151.

M259

Figure 10: M259 milling a surface in a hydro electric power station.

Construction year	1998
Approximate weight	6000 - 8000kg
Minimum working diameter	3000mm
Maximum working diameter	9000mm
Minimum height	1100mm
Number of legs	6

Table 2: Physical attributes M259.

2.6. The M391 Circular Milling Machine

In 2008, Wagner GmbH commissioned the construction of a third circular milling machine, namely machine M391. In addition, discussions were held between the University of Cape Town and Wagner GmbH concerning a joint co-operation. This resulted in the project at hand, whereby facilitated research would be conducted into the field of circular milling concerning repeatability and accuracy. The findings of this research and the resulting design concepts would be combined with the technical experience gained by Wagner GmbH in the prior fifteen years to form the basis for a new generation circular milling machine.

The new M391 circular mill was intended to operate over a range of diameters that intersected with both machines, allowing increased performance at larger diameters with the gained advantage of reduced weight. Table 3 illustrates the ranges of operation for the M151, M259 and M391 machines.

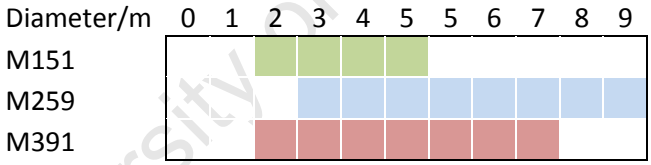

Table 3: Operating diameters for the Wagner GmbH circular mills.

2.7. Industrial Circular Mills

There are three main competitors to the existing Wagner GmbH circular mills as listed below. They too operate in the ϕ2m to ϕ10m flange surfacing range. Limited data is made available on these machines. However, relevance pertaining to each is compiled as per below.

SILK – AX48-120 Flange Facer [3].

The AX48-120, illustrated in Figure 11, is designed to be a flange turning device although an orbital milling kit is available. The flange range is from ϕ1219mm to ϕ3429mm with a shipping weight of 1445kg. A novel feature of this machine is that the adjustment for alignment is between the top plate and base rather than at the feet. The machine uses 8 legs which are segmented with feet that adjust in the radial direction. The operating diameter is adjusted by altering the position of the arm as well as linear slides on the arm.

Figure 11: SILK AX48-120 flange facer [3].

Climax Portable Machine Tools Inc.- CM6000 [4].

The CM6000, illustrated in Figure 12, from Climax Portable Machine Tools Inc. is a portable circular milling machine that operates over a milling diameter range of ϕ1993.9mm to ϕ5003.8mm with a shipping weight of 6350kg. The mounting diameter is adjustable with the 8 segmented legs. Adjustment for alignment is performed at the feet with adjustment in the radial and axial directions hereby made possible. Rotation is enabled by means of a slewing bearing mounted to the base of the machine. Working diameters adjustment is attained with adjustments to the radial arm position as well as the radial slide onto which the tool is attached. The machine has a claimed accuracy of $^{+}/_{-}$ 0.032mm/m

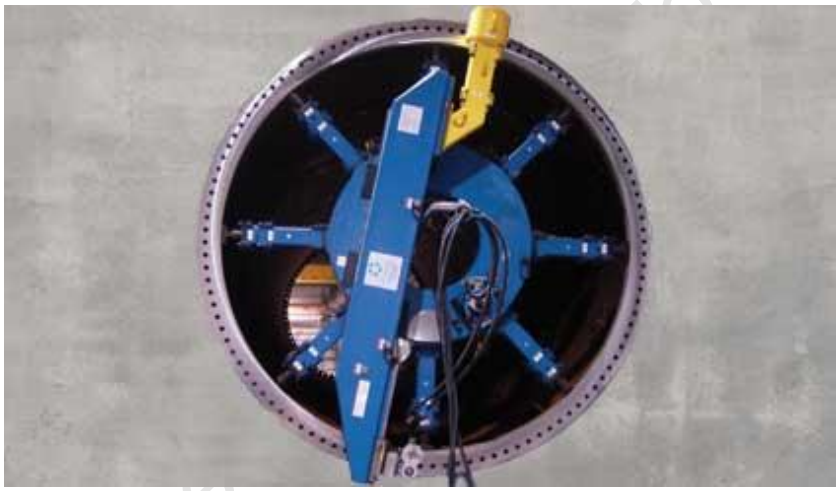

Figure 12: Climax CM6000 [4].

Self Levelling Machines Pty Ltd – CSLM [5]

The Self Levelling Machines Pty Ltd – Circular Self Levelling Machine, illustrated in Figure 13, operates on a unique principle. Instead of using a large, slewing type bearing to support the arms, the arms are attached to a central pivot post. The arms and milling head are supported on wheels that roll on the surface being machined. These machines are designed to machine horizontal or near horizontal surfaces of diameters from approximately ϕ2000mm to ϕ9000mm. The larger XL-CSLM uses a similar principle although the tool cuts a flat plane because the wheels are controlled to maintain the tool in a level plane by referencing from a central scanning laser. The XL-CSLM operates between approximately ϕ6000mm and ϕ50 000mm.

Figure 13: SLM Circular self levelling machine [5].

2.8. Current Design Features

With circular milling machines, the working diameter of the machine is varied in almost every job. This means that the machine must be able to both operate on and mount to the work over a range of diameters. The mounting has always been done using segmented legs, whereby a combination of leg segments of varied lengths are paired with the feet in order to attain a set diameter. This concept has been adopted in the past by both Wagner GmbH and other reputable portable machine builders.

The selection of working diameter is similar. There are three factors that effect the radial position of the tool and hence the working diameter.

- The position of the arm relative to the base of the machine.
- The length of the arm segments.
- The position of the radial slide mechanism.

The M151 machine utilises two available arm segments, one of 950 mm and another of 1400 mm. The larger is mounted directly to the base and the position of this mounting can be varied which will in turn effect the working diameter. Figure 14 illustrates the base of the M151 with the arm removed, consisting of holes along the sides of the bare metal strip that are used to mount the arm. In order to attain larger diameters, the smaller arm extension is attached between the arm end and the milling head assembly.

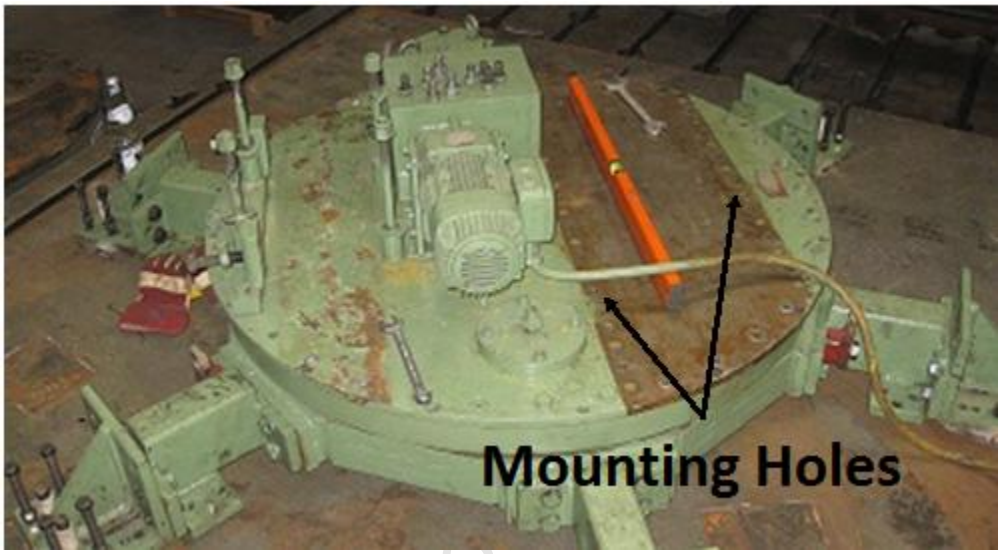

Figure 14: Base of M151 with arm removed.

The M259 uses a similar configuration. With arm segments of 2550mm the large machine can mill up to 9000mm. Both machines are assembled with the arm being mounted across the whole surface of the base, i.e. from edge to edge of the base, this can be seen in Figure 14. The arm of the M259 positioned along the centre of the machine and the M151 arm is offset 400mm from the centre. These mobile machines have to be assembled on-site before operation.

It is essential that the tool be perfectly perpendicular to the surface during operation. In order to ensure that the tool remains perpendicular each time the machine is assembled, the interface between the arm, arm extenders and milling head assembly incorporate two perpendicular feather keys located in toleranced keyways. It has been assumed in the past that the tool is perpendicular when assembled as a result of the manufacturing process, although machinists have noted that this is not true.

The legs of the M151 are secured to the base by means of 4 x M20 screws and the M259 6 x M20 screws in a rectangular pattern. The DIN 20373 [6] standard states that the clearance holes for a M20 screw should be ϕ22mm, which means that each joint between segments can introduce $^{+}/_{-}$1mm or 2mm uncertainty in terms of the position of the legs. The M259 legs have a single dowel pin located in the centre of the interface. While this does provide a higher degree of locational certainty the leg is still able to rotate about the pin.

The current measurement protocols do not account for the position of the legs relative to the machine. This is to be illustrated later in the text, demonstrating that misalignment of the feet has a direct effect on the bearing. Since the legs are not located relative to the base of the machine, it is not possible with the current machines to measure the positions and prevent misalignment.

The feet used on the M151 illustrated in Figure 15 utilize two M36 x 2mm set screws (2) to raise the foot and four M20 bolts (1) to secure the foot to the plate that is welded to the work. This system allows for the foot to be adjusted by up to 40mm. Although this foot effectively uses six points that can effect the position of the leg, it is possible to induce a rotations moment on the leg if the bolts and screws are tensioned dissimilarly. The foot of the M259 shown in Figure 16 is an improvement on this system as there are four tensioning bolts (a) that secure the foot to an adjustable taper block (b). The taper block uses a tapered retractable component that mates with another fixed tapered component. Adjusting the retractable component in effect alters the height of the foot. This system is an improvement over the M151 although is time consuming to use.

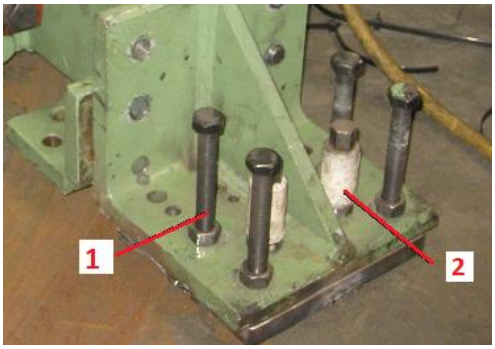

Figure 15: M151 foot.

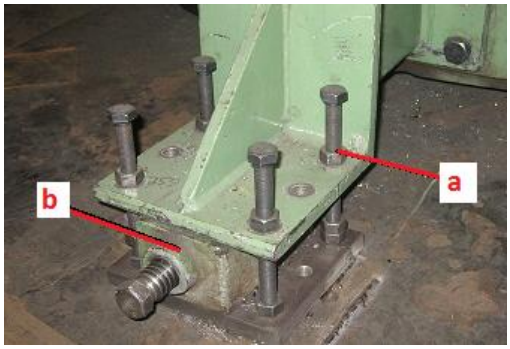

Figure 16: M259 foot.

2.9. Flange Deformation and Un-Flatness.

Flanges are in essence flat circular surfaces. They are used for mounting load carrying elements such as bearings, or for joining structural elements. When they are used for mounting precision elements such as slewing bearings, the mounting surfaces are required to be machined to within an un-flatness tolerance.

The un-flatness tolerance P, illustrated in Figure 17, is used to prevent shape defects in the bearing. This un-flatness tolerance includes the taper error which is defined as the difference in the height between the inner and outer diameters of the surface as shown in Figure 18.

Figure 17: Two planes representing the total un-flatness of a flange.

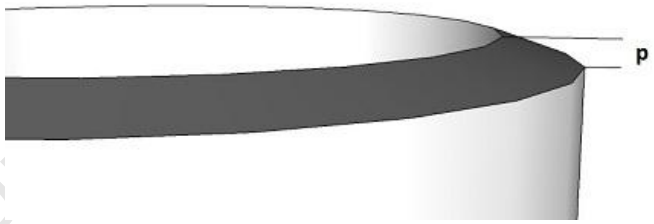

Figure 18: Illustration of taper error of a flange.

Shape defects of the supporting structure lead to deformation of the bearing raceway. This can cause irregular stress distributions or localised stresses and will thus reduce the bearing lifespan [7]. Each bearing manufacturer has its own specific un-flatness limits. These are defined over the range of manufactured bearings. The values provided in Table 4 below are taken from the Rothe-Erde slewing bearing catalogue [8].

Track diameter in mm D_t	Out-of-flatness including slope per support surface "P" in mm		
	Double row ball bearing slew ring axial ball bearing	Single row ball bearing slewing ring 4 point contact bearing* double 4 point contact baring	Roller bearing slewing ring Combination bearing
to 500	0.15	0.10	0.07
to 1000	0.20	0.15	0.10
to 1500	0.25	0.19	0.12
to 2000	0.30	0.22	0.15
to 2500	0.35	0.25	0.17
to 4000	0.40	0.30	0.20
to 6000	0.50	0.40	0.30
to 8000	0.60	0.50	0.40

Table 4: Rothe Erde un-flatness values [8].

These values are of importance to both the final outcome of the on-site machining process and the design in this project. Both of the current Wagner GmbH circular mills use slewing bearings as the main load carrying device. Similarly, the new Wagner GmbH M391 machine will use a slewing bearing.

These bearings are designed to be mounted to rigid companion structures. The purpose of the slewing bearing is to transfer load from the turntable of the structure to the chassis. Some manufacturers include a second set of tolerances termed the stiffness tolerance. These represent the deflections of the companion structure during operation. Illustrated in Table 5 is the guideline set out by Global Bearing Services [7] with regards to stiffness tolerances.

Raceway average (mm)	500	750	1000	1250	1500	2000	2500	3000	4000	5000	6000
Max Deflection (mm)	0,25	0,30	0,35	0,40	0,55	0,65	0,81	1,00	1,25	1,80	2,4

Table 5: Global Bearing Services stiffness tolerances [7].

The slewing bearings are fixed to the companion structure via tensioned bolts. The bearings are designed to be load transferring components that rely on the rigidity of the companion structure for support in preventing deformation. Since the companion structure is significantly more rigid than the bearing, it will take the form of the structure it is mounted to. Deformation in the roller raceway leads to greatly increased contact stresses and in turn reduces the lifespan of the bearing.

2.10. Cutting Forces

The cutting torque and power are defined as the torque required in rotating the tool during engaged cutting and the power requirement thereof. The three dimensional cutting forces were calculated as follows:

The cutting force (F_c) is calculated using an empirical data based formula [6]. The method used incorporates results from previous tests into a cutting force per unit cutting area (k_c).

$$F_c = A \times k_c \quad \textbf{(1)}$$

This cutting force represents the force per engaged tooth in the direction of rotation. This data is based on a face milling tool with 0° axial rake and +6° radial rake. Since the geometry of the tool used is different to that used in calculating F_c it is necessary to calculate a value that excludes the effects of the geometry, which subsequently allows the effects of the new geometry to be incorporated. The shear plane model for orthogonal cutting [9] presented in equations (2), (3) and (4) combines a nominal force with the geometric factors of the cutting process in order to resolve the forces into three dimensions as illustrated in Figure 19:

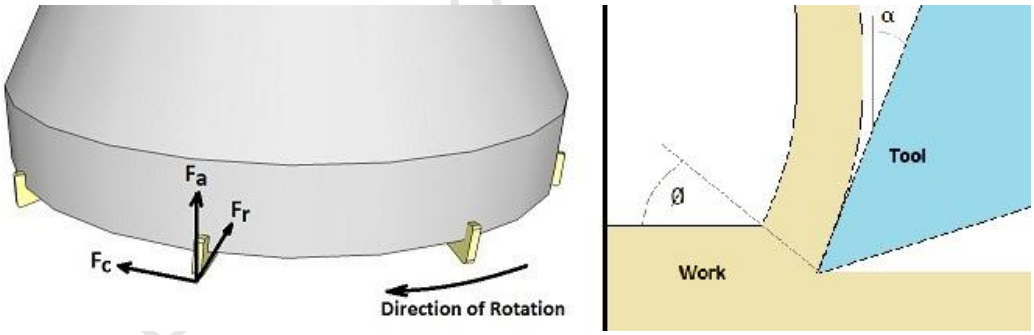

Figure 19: Forces acting on work relative to tool insert and cutting geometry.

Cutting

$$\mathrm{F_c} = \mathrm{k} \times \mathrm{a} \times \mathrm{b} \times \frac{[\cos(\beta - \alpha)\cos\lambda + \sin\beta \sin\lambda \tan\eta]}{\sin\emptyset \cos(\emptyset + \beta - \alpha)} \quad \textbf{(2)}$$

Radial

$$\mathrm{F_r} = \mathrm{k} \times \mathrm{a} \times \mathrm{b} \times \frac{\sin(\beta - \alpha)}{\sin\emptyset \cos(\emptyset + \beta - \alpha)} \quad \textbf{(3)}$$

Axial

$$\mathrm{F_a} = \mathrm{k} \times \mathrm{a} \times \mathrm{b} \times \frac{[\cos(\beta - \alpha)\sin\lambda - \sin\beta \cos\lambda \tan\eta]}{\sin\emptyset \cos(\emptyset + \beta - \alpha)} \quad \textbf{(4)}$$

where the rake angle α, inclination angle λ and cutting force F_c are known. The friction angle β, shear angle ϕ and chip flow angle η need to be calculated. The model presented by Toropov-Ko [10] is used to predict the shear angle ϕ:

$$\emptyset = \frac{5}{8}\alpha + \frac{1}{2}\text{acos}\left[e^{\left(-52.5\times10^{3}\left(\frac{\sigma_u}{100\rho c}\right)^{0.8}\left(va\times\frac{10^{3}}{\omega 60}\right)^{0.4}\right)}\right] \quad \textbf{(5)}$$

where, σ_u is ultimate tensile stress, ρc is the product of density and specific heat, v is cutting speed, a un-deformed chip thickness and ω is thermal conductivity. The Toropov-Ko method was used since it allows for the shear angle to be calculated from the thermo-mechanical constants of the material without the need for extensive testing of the material.

Using the Stabler relation for chip flow for oblique cutting it is therefore possible to calculate the friction angle β [11]. The relationship between chip flow angle and inclination set out by the Stabler model is also applicably used as per below:

$$\emptyset = 45 - 0.5(\beta - \alpha) - 0.5\beta \quad \textbf{(6)}$$

where

$$\eta = \lambda \quad \textbf{(7)}$$

The product of the flow stress k and the chip cross section a×b is calculated from equation (2). This k×a×b value combined with the correct tool geometry in equations (2), (3) and (4), which generates the forces per tooth. The values from the engaged teeth are then resolved with respect to the machine coordinate system.

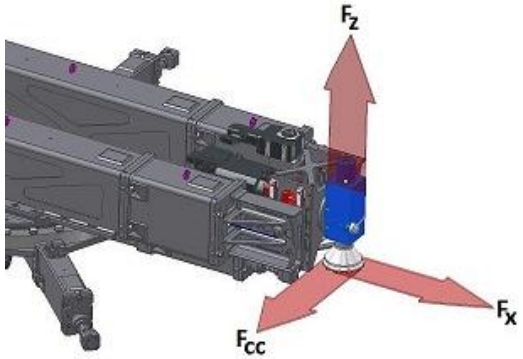

Figure 20: Resultant cutting forces on work relative to milling machine.

3. Metrology

3.1. Methods of Measuring Machined Surface Quality.

3.1.1. Industrial Metrology: Surfaces and Roundness[12]

When analysing machining processes it is important to be able to compare the outcome of each accordingly. In terms of a face milling process, the outcome is a machined surface so it would therefore follow that in comparing processes or machines, the produced surface would be compared.

In order to compare the surfaces, it is first necessary to identify the features of that surface and quantify them, thus allowing a fair numeric comparison. The texture of a surface as illustrated in Figure 21: The major components of a typical surface texture is a complex combination of the following three features:

- Roughness profile– comprising of irregularities that occur due to the mechanism of the material removal process or tool geometry. A common value for representing the roughness is R_a. The subscript "a" represents the arithmetic mean of the absolute values for the roughness measurements

- Waviness profile – that component of the surface texture upon which roughness is superimposed, resulting from factors such as machine or part deflections, vibrations and chatter; material strain and extraneous effects. The characteristic value used to represent the waviness is W_a.

- Primary profile – the overall shape or the surface – ignoring roughness and waviness errors in machining tool slide ways. The measurement used to quantify the primary profile is the height of the profile P_t, or total un-flatness P. This measurement is the difference between the highest point and the lowest point on the profile.

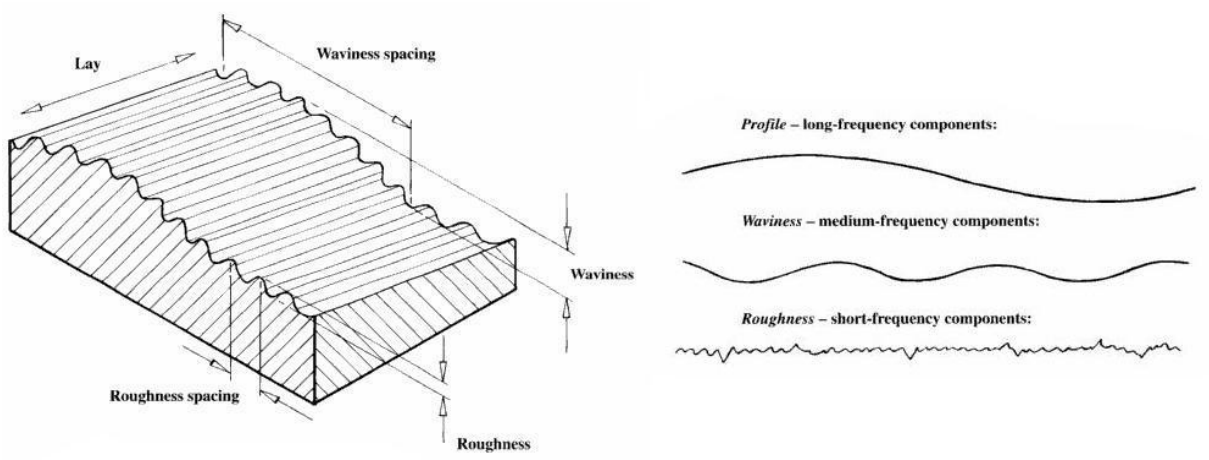

Figure 21: The major components of a typical surface texture [12].

There is a fourth condition referred to as the “lay” of the texture. This is the direction of the dominant pattern resulting from the milling process. Surfaces generated by milling are topographically anisotropic where the surface properties are statistically dependent on measurement direction [13]. The defined tool geometry in milling generates severe anisotropic patterns. This can be increase when the tool is incorrectly aligned to the surface, causing the leading or trailing inserts to produce clearly defined lay. Figure 21 illustrates an example of a surface topography demonstrating anisotropic lay. The measurements of roughness are taken perpendicular to the dominant lay direction.

Digital Levelling [14][15]

The digital level used for assessing change in vertical height was the DiNi 11 from Carl Zeiss. The device utilises an invar-type staff that is placed symmetrically to the line of sight. The device requires that 30cm of the staff be visible.

The device has a standard deviation of 0.01mm when measuring at distances less than 10 m. The digital level is placed on a tripod as illustrated in Figure 22. Once mounted the device is levelled out using three extending screws that adjust the attitude. Once levelled the device can be rotated through an angle of 360° parallel to the horizon. The Invar-type staff is placed on the surface by means of a pivoting magnetic base that allows the staff to remain vertical.

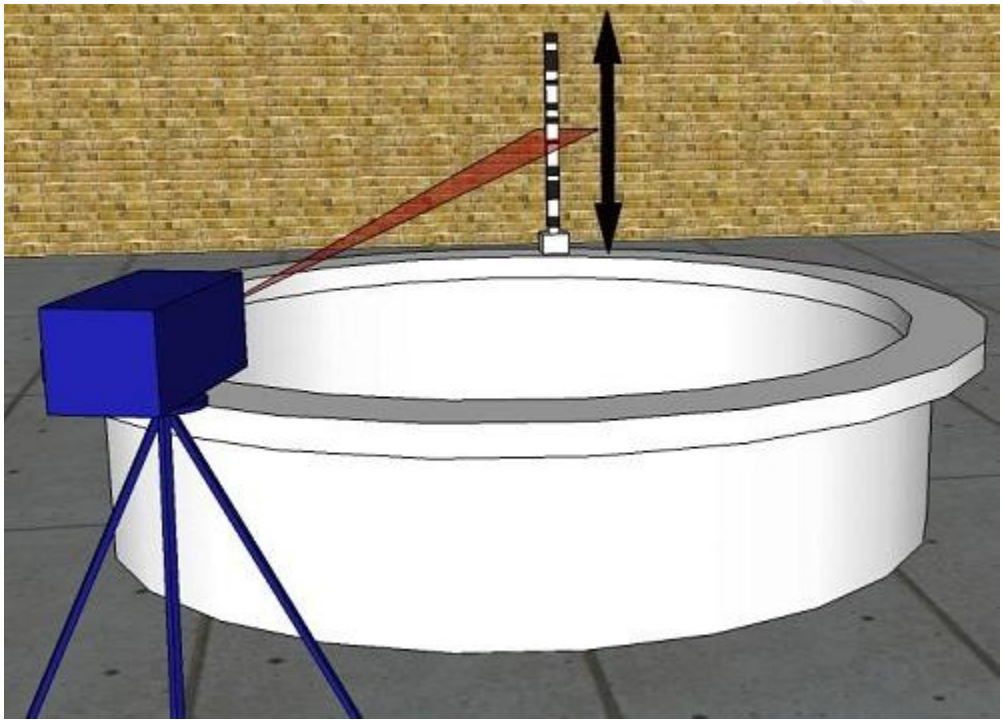

Figure 22: Representation of the digital levelling process.

By placing the staff at points around the flange, it is hereby possible to measure the primary profile produced by the engaged tool. By placing the staff on the milling head assembly and rotating the machine it is also possible to measure the orbital path of the tool.

Dial Gauge

The dial gauge is used to accurately measure linear distances. They are small devices that can be easily mounted to a machine. They are secured by a magnetic base with an adjustable arm. By combining the adjustable arm and magnetic base, the dial gauge is position able perpendicular to the surface being measured. Thereafter, depending on the setup attained, either the work is moved in a direction perpendicular to the desired measurement direction, or the machine is moved relative to the work.

Figure 23 illustrates a dial gauge mounted to the spindle of a vertical milling machine via a magnetic base. The dial gauge is positioned perpendicular to the surface being measured. The gear is mounted to a rotatable table. This table is then rotated and the height relative to the machine spindle is thus measured. Herewith, the gauge is being used to ensure that the surface is parallel to the machine table onto which the gear is mounted.

Figure 23: Dial gauge measuring flatness of a gear mounted to a milling machine.

The dial gauges used at Wagner GmbH are accurate to 0.01mm which is sufficient for the in-house and on-site milling activities. The instrument is mounted to the machine and assumes perfect or near perfect machine raceways. The measurement accuracy is independent of the range of the measurement.

In practice, these gauges are mounted to the circular milling machine, near or on the milling tool itself and the machine is thereafter rotated so that the profile of the flange can be measured. The co-ordinate system for this method of measurement is relative to the machine. If the machine raceways are distorted or damaged, the outcome of the measurement will be effected.

3.2. Current Measurement and Alignment Protocols

The objective of the circular milling process is to remove material from an existing surface in such a manner that the final surface achieved is to that of the customer requirement, as well as ensuring the surface quality and total un-flatness are within the prescribed tolerances. Occasionally there is the further constraint that the produced flange should be concentric and/or parallel with some external reference surface or axis.

In order to produce the required surfaces, it is necessary to set the machines up to operate within tolerance. Since these machines are mobile, they need to be set up each time for each new job. This poses a problem since the references can be from different places relative to the machine each time the machine is set up.

In order to ensure that the machines are set up correctly each time there are protocols set out by Wagner GmbH for the machinists to follow. There are no international standard protocols available, this could be due to the short time that the industry has been active or the secrecy that the competitive market creates. These are general guidelines and sometimes need to be altered to meet the requirements of the job.

The current methods of setting the machine require the use of a dial gauge and measurement of the flange surface or adjacent surfaces relative to the machine. These measurements are dependent on the alignment and geometry of the adjacent or pre-existing surfaces. The assumption made is that the reference used to align the machine is perfectly orientated in space. This assumption is used unless the customer requests or is able to provide an absolute reference.

It is possible that when the chosen reference is flawed or misaligned, the machine can be set up so that it appears that the orientation is within tolerance, but in fact is not. In order to understand the possible outcomes and downfalls of this technique, the two primary measurement protocols at Wagner GmbH are set out below.

3.3. Protocol 1

The machine is positioned on the work with a crane. While still suspended from the crane, rough measurements are taken with a tape measure. Using these measurements the feet are positioned radially and axially so that the machine is approximately in the centre and parallel. These measurements are typically accurate to within +/–5mm. Once this approximate setup is attained, half of the feet are secured in alternate positions of the mounting surface. The positions of the first feet to be initially fastened are shown in Figure 24, i.e. 1, 3 and 5.

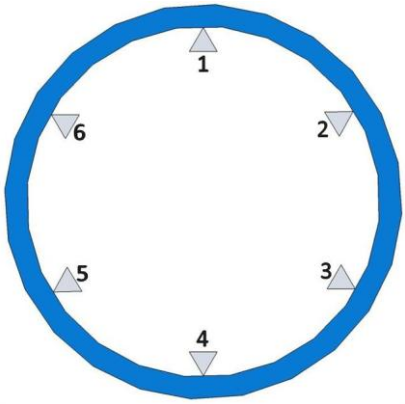

Figure 24: Top view of the mounting positions of the feet with the M151 and M259.

Once the first set of feet are secured, a dial gauge is mounted to the milling head and oriented such that it measures the change in height of the flange relative to the milling head in the z direction. The first step is to measure the z height at points 1, 3, 5 on the surface. The objective is to align the mill in order for these three points to form a plane that is parallel to the desired plane. This is achieved by selecting one foot as the reference and adjusting the others to the same height.

The next step is to align for concentricity. For this the dial gauge is placed on a cylindrical reference surface, oriented to measure the cylindrical reference surface in the radial direction. The x-axis value is measured at the three secured points, followed by radial adjustment at these points so that the x-axis value is the same relative to the cylindrical reference.

At this point the machine has been adjusted for parallelism and concentricity using alternate legs. These alternate legs carry the full weight of the circular mill. The remaining legs are suspended in space. This means that relative to the secured legs, they hang, which in turn introduces stresses on the bearing.

The final stage of adjustment is to secure the remaining legs so that each leg shares the load of the machine equally. This action also reduces the induced stresses on the bearing, resulting in the bearing returning to its unstressed shape. Thus the cutting plane will come into tolerance. Before this final adjustment, the path followed by the tool is approximately sinusoidal in the Z-direction as the arm of the machine traverses over each supported and unsupported leg section.

3.4. Protocol 2

This method uses a cylindrical reference surface for finding both concentricity and parallelism. As with method one, the machine is mounted in an approximately correct position and then alternate legs are secured.

Once the machine is mounted in its initial position, the machine is set up for concentricity. As before, this is done with the dial gauge oriented radially measuring the position of the machine relative to a cylindrical reference.

The next step is to attach the dial gauge so that it still measures the position in the radial direction but can be adjusted so that it measures this in two axial positions relative to the cylindrical reference surface. The accuracy of this method is directly effected by the length of the cylindrical surface used. This is illustrated below in Figure 25.

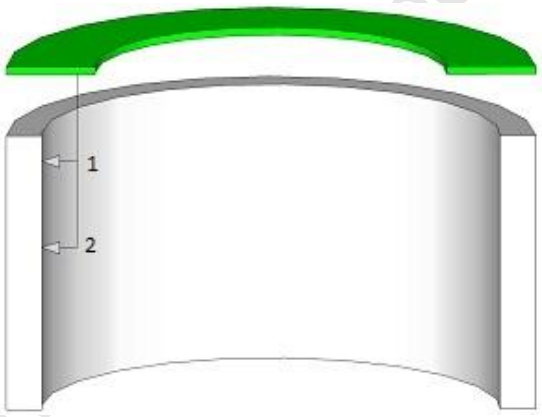

Figure 25: Illustration of protocol 2.

When the values at position one and two remain the same, the process is repeated with the arm positioned at 90° to the initial position. The alignment, in two perpendicular directions, ensures that the cutting plane is orthogonal to the central axis of the cylindrical reference surface. Adjusting at 90° adjusts the machine about two axes, although requires that two legs be used for one axis and four for the second. Adjusting about two axes is faster than about three, although doing so with six legs is not practical.

3.5. Downfalls of Existing Protocols

The first method sets the machine up in a plane that is approximately parallel to the existing flange, although this is dependent on the existent deformation in the flange. If the un-machined flange surface is severely deformed from welding, damaged or misaligned, then this plane could be in an undesirable orientation relative to the desired flange. This is illustrated in Figure 26 where a surface orthogonal to the central axis of the cylindrical referance is desired but a surface parallel to the existing surface is acquired.

Figure 26: Orientation relative to flange (side view).

The second method can correct the potential error illustrated in Figure 26 and is often used when there is a need for the final surface to be aligned orthogonal to the central axis of to a plane perpendicular to some cylindrical reference. However, this is not possible when there is no cylindrical reference nearby that can be used as a reference. As illustrated in Figure 27, the second method rules out the possibility of measuring the relative distance between the tool and existing surface, making it difficult to control the un-flatness outcome of the milling process since there is only indirect control over the tool position.

Figure 27: Orientation relative to axis.

3.6. False Method

Although the setup protocols are set out as guidelines for proper machine usage, these have not always been followed. The method that is most common can be referred to as the false or zero difference method. The user endeavours to set the machine up so that each measurement reflects the same z value on the dial gauge at each position of measurement around the surface.

While this method may deem appealing, it is important to remember that the customer would not have requested a flange be worked on if it were already within tolerance. When the users set the machine up in this manner they could use the same adjustment sequence as the first protocol method. Furthermore, they measure the height of two opposite points on the surface and adjust them followed by the two perpendicular points. Although the fundamental difference with the false method is that the measurement at all eight (or 6) points will show the same value (e.g., 0.00mm), forcing the tool to follow the profile of the existing surface.

When the machine is set up like this, it no longer pivots around the two perpendicular feet. The feet will align with the surface and induce stresses on the machine that are unnecessary since the arms are in effect opposing each other by pushing in different directions.

With this method, the user will view a reading on the dial gauge that reflects zero change in the axial height of the flange. This means that the machine head is always moving approximately parallel to the existing surface. The problem is highlighted when looking at this situation in terms of the absolute coordinate system. Figure 28 illustrates this where the flange, represented by the blue surface has an axial height that varies sinusoidally around the flange. The red surface represents the cutting plane. Since the tool is maintaining a constant distance away from the flange, the path is no longer planar.

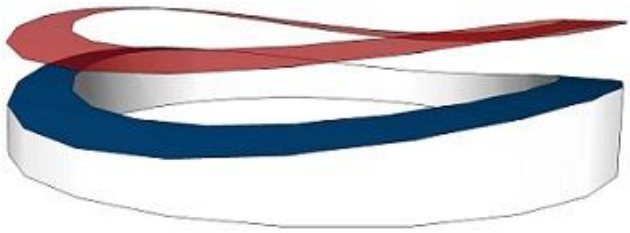

Figure 28: False alignment of the cutting plane with the existing surface.

3.7. Deflection Simulation

3.7.1. Description of Deflection Simulation

In order to demonstrate the effect that the false method or poor setup practice has on the bearing, the following simple simulation was devised. Figure 29 illustrates the simulation with 8 arms of DIN 10210 120x80x12.5mm profile (used on the current machine legs) at ϕ4000mm combined with a ϕ 1200 - ϕ1400mm ring 100mm thick, material S355 J2+N. The ring has two rows of ϕ24mm holes and represents a simplified version of a slewing bearing. Four of the legs at positions 1, 2, 5 and 6 are fixed at the outer end with movement constraints in all directions. The legs at positions 3, 4, 7 and 8 are deflected downwards by 3.2mm by a force of 10 000N acting parallel to gravity on each of the leg ends. The effects of gravity were included in the simulation.

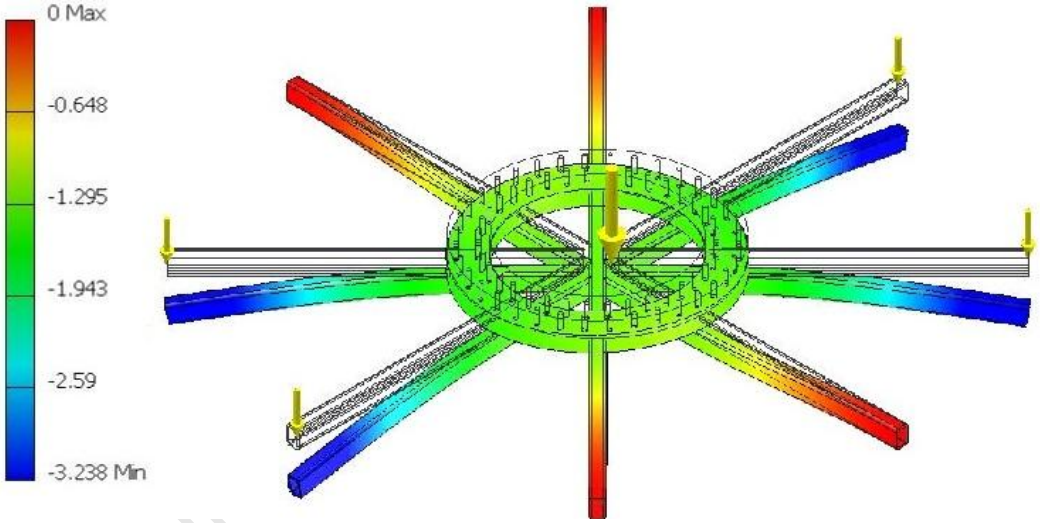

Figure 29: Deflection simulation model.

The deflection of the bearing was measured at 16 equally spaced points around the bearing corresponding to the points of intersection of the centre of each leg and the outer diameter of the bearing as well as the points halfway between each leg on the outer diameter. This simulation excludes the plate that is attached to the upper bearing surface in order to demonstrate the susceptibility of the bearing to deformation.

3.7.2. Results of Deflection Simulation

The maximum downward deflection corresponding to the points between legs 3 & 4 and 7 & 8 was **-1.21mm**

The minimum downward deflection corresponding to the points between legs 1 & 2 and 5 & 6 was -**0.898mm**

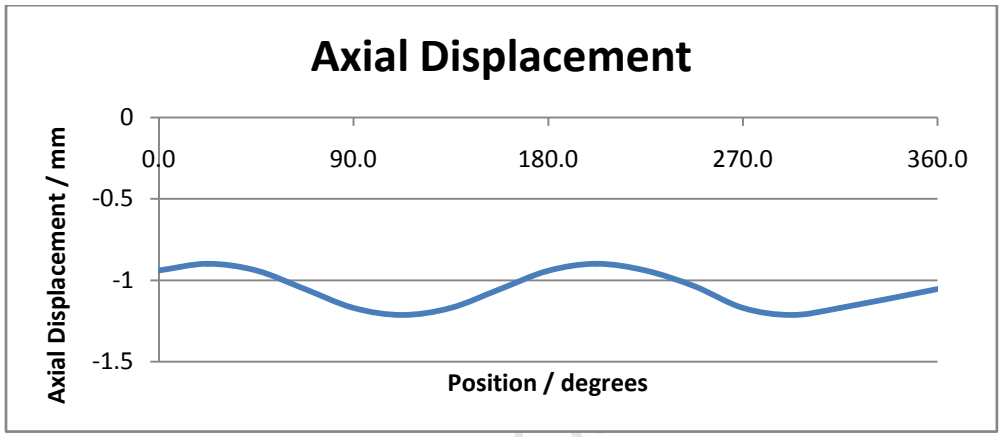

Figure 30: Deflection of slewing bearing under poor setup conditions.

This produces an un-flatness measurement of **0.315mm** over the bearing surface. As illustrated in Figure 30, the bearing is deformed in an approximately sinusoidal manner relative to the Z-axis. The bearing used in the construction of the M391 machine was a single row crossed cylindrical roller slewing bearing with an un-flatness tolerance of 0.2mm.

The slewing bearings used in the construction of circular mills are designed to be pared with distortion resistant companion structures. Figure 31 illustrates an example of a slewing bearing support structure which is mounted to the upper race of a slewing bearing in order to provide rigidity and to prevent the bearing from deforming in a manner that could cause damage. The support shown was 450mm high and had internal and external diameters of ϕ1200mm and ϕ1400mm respectively.

Figure 31: Slewing bearing support structure.

With this in mind it is important to remember that circular mills are portable machines. It is not desirable for the machine to use such a companion structure where the weight is approximately 1.5tons. These passive structural dimensions also prohibit their use in portable machines using slewing bearings. Some jobs require that the overall height of the machine be kept as low as possible, again preventing the use of these components.

Figure 32 illustrates an example where the rotating section of a harbour crane is elevated by hydraulic lifts. The circular milling machine is fixed to the lower surface but aligned with the upper surface. In this case the height of the machine is critical. Once the hydraulic cylinders are extended, hard wood sleepers are used to support the structure. The high cost of these sleepers restricts the allowable height that the structure can be elevated; often the maximum elevation attainable is 600mm.

Figure 32: Inverted milling of a harbour crane upper bearing seating.

These restrictions on the overall height of the construction of the circular mill prevent the use of support structures being used that would increase the height of the machine. This factor emphasises the importance of the alignment and setup capabilities since it is not possible to use companion structures that force stability and ensure the bearing is correctly oriented.

3.8. Current Evaluation

Currently, the rotations lasers or digital levels are used for the initial evaluation of the existing surface and then again with the evaluation of the outcome. As stated previously, the measurements used for aligning the circular milling machine to the work are relative to the machine.

The laser measurements can be viewed as being in an absolute frame since the laser reference will remain fixed in space throughout the process. Using the dial gauge between the milling head and surface, as illustrated in Figure 33, is a relative measurement. Combining these two methods as is done in the current protocols introduces a discontinuity in the measurement process that causes uncertainty in the final result. Relative measurement between the work and the tool also has the disadvantage that the work geometry is altered after each pass of the tool.

Figure 33: Dial gauge measuring between the milling head and surface.

This uncertainty is sometimes counteracted by performing intermittent measurements with the absolute measurement systems, thus allowing for adjustments to be made to the alignment before the final cut is performed. However, this is deemed time consuming and it is not desirable to adjust the machine after it has been secured.

Since the precision electronic measurement devices are sensitive to external vibrations, it is not always possible to use them in the field. Furthermore, it was desirable to create a system that would allow for in-situ measurement as well as increasing the accuracy of the alignment process.

As discussed prior, it is possible to alter the setup configuration so that the bearing is bent out of tolerance. The bearing in effect lies directly on the plane created by the legs. By adjusting the legs this plane can be altered and in turn the bearing and the profile of the tool are controlled. From this it can be seen that having control over the legs and more certainty of their position in space will be beneficial in the setup process. This subject is addressed later in this report.

4. Methodology

4.1. Aim

The objective of the tests was to investigate the relationship between setup process and the final outcome in the milling process. In the first set of tests the machines were set up to operate within tolerance at a set diameter of ϕ3500mm. The unengaged tool profile was recorded and compared to the profile produced by the fully engaged tool on the surface.

The same process was followed with the second set of tests, although the machines were set up to investigate the potential for a limit to the achievable accuracy in the process. An absolute reference measurement system was used in all tests and this was compared to the relative measurement systems.

4.2. Test Conditions

In the tests both the M151 and the M259 were used. The two machines were set up to mill at a diameter of ϕ3500mm. It was important that this diameter was also attainable by the M391 as it would be tested in the same manner once constructed.

The machines were mounted to a 2500mmx4000mm S355 J2 +N steel plate which was secured to the bed of a vertical milling machine. This setup, shown in Figure 34 did not allow for the milling of a complete orbit. 36 measurement points were used per orbit. 11 points were engaged with the M151 and 9 with the M259.

Figure 34: M151 during testing phase.

A horizontal reference plane was used and the machine cutting planes were set up to be parallel to this. The measurement of vertical height was achieved with the aid of a digital levelling device accurate to 0.01mm having. The staff used a magnetic base with a pivoting joint, illustrated in Figure 35. This pivoting joint combined with a spirit level ensured that the staff remained vertical within $^{+}/_{-}$ 2° in each new arm position.

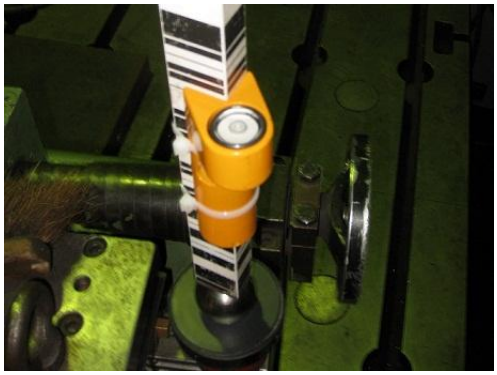

Figure 35: Magnetic base, pivoting joint and staff used for measurements.

The measurements of the unengaged profile were achieved by attaching the staff to a fixed surface on the arm of the circular mill at the same diameter as the tool. The machine was rotated through the orbit with measurements being taken at the 36 equally spaced intervals. Measurements of the surface profile were made by placing the staff on marked positions on the surface correlating to the points measured of the unengaged profile.

The conditions selected in Table 6 and Table 7 were chose such that the machines would operate chatter free. The following cutting conditions were used in the tests:

M151

Tool diameter	200 mm
Number of inserts	11
Cutting speed	approx 190 mm/min
Spindle speed	300 rpm
Feed speed	330 mm/min
Cutting depth	0.1 – 0.3 mm

Table 6: M151 testing conditions.

M259

Tool diameter	80 mm
Number of inserts	5
Cutting speed	approx 360 m/min
Spindle speed	1432 rpm
Feed speed	716 mm/min
Cutting depth	0.1 – 0.3 mm

Table 7: M259 testing conditions.

4.3. Milling Tests

4.3.1. Test 1: In Tolerance Opperation

The first test entailed setting up the M151 and M259 to operate within tolerance at the operating diameter of ϕ3500mm. The tolerance used was for a crossed cylindrical roller slewing bearing and was between 0.17mm and 0.20mm [8]. The machine was set up using the first measurement protocol with the exception of the relative measurement system used as discussed before.

The initial phase was to set up the machines on the alternate legs so that the profile of the tool was within tolerance at the secured leg positions. At this time interim measurements were taken at points corresponding to the alternately secured legs to demonstrate the sinusoidal profile (as stated on page 33). Figure 36 illustrates the plate used to secure the feet of the M151 to the work with the left side being elevated and the right resting on the surface of the work illustrating the subtle difference between the supported and unsupported feet. These plates are welded to the work before being adjusted.

Figure 36: Comparison between the supported and non supported feet.

When approximate orientation was attained with the initially secured feet, the remaining feet were secured and brought into a load carrying state. At this point it was necessary to measure the points corresponding to all of the legs, i.e. six with the M151 and eight with the M259. Once the measurements at the points corresponding to each leg were within tolerance, the machine

was considered to be aligned. The profile traversed by the tool during unengaged orbit was then measured.

Once the machine was aligned and the unengaged profile was measured, the surface could be milled. This was accomplished by ensuring that the tool was fully engaged throughout the entire arc of the surface. If engagement was interrupted the process was repeated until the tool remained engaged throughout the arc. For cutting passes whereby the surface was to be measured, the cutting process was treated as a finishing pass with maximum 0.1mm cutting depth. This, as a result, produced a higher quality surface texture as well as prevented chatter.

4.3.2. Test 2: Achievable Performance

The second test was performed as an improvement on the set up from the first test. The objective here was to set up the machines to that of total un-flatness between the points corresponding to each leg that was less than the total un-flatness around the orbit. This would isolate the characteristic features introduced by the machine excluding the effect of setup.

The same technique was used with the digital levelling device measuring the positions of the arm in orbit. This was followed with multiple finishing cuts of 0.1mm to ensure the tool remained fully engaged across the entire surface. Figure 37 illustrates the resulting surface from test 2 with the M151 circular mill.

Figure 37: M151 milled surface from Test 2.

4.4. Results of Milling Tests

4.4.1. Setup With Alternate Legs Secured

As stated, measurements were taken of the vertical position of the arm corresponding to each leg when alternate legs were fixed. In this position, the slewing bearing was stretched such that the unengaged orbit was out of tolerance. The plots in Figure 38 and Figure 39 below illustrate these measurements for the M151 and M259 respectively.

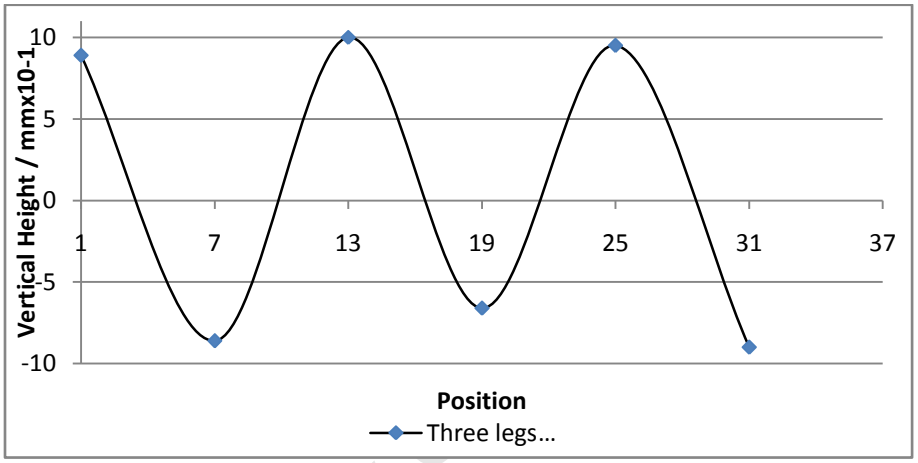

Figure 38: M151 setup profile with three legs secured.

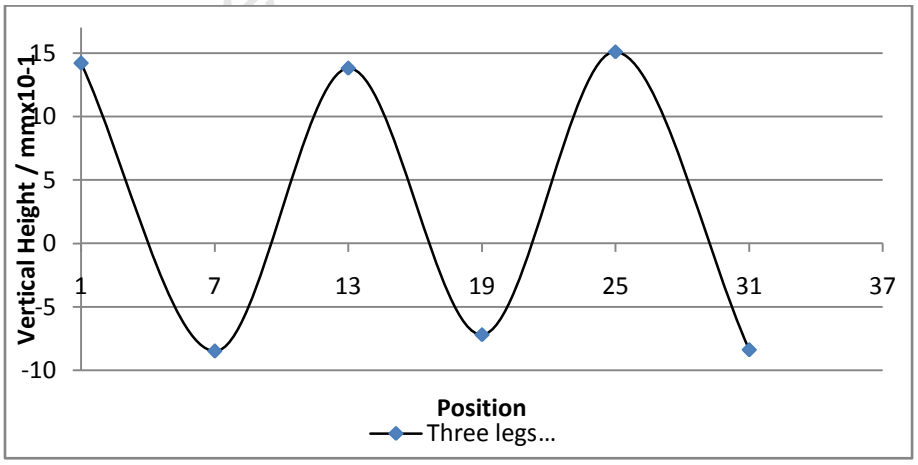

Figure 39: M259 setup profile with three legs secured.

4.4.2. Test 1 Results

Figure 40 and Figure 41 represent the findings of the first set of milling tests where the machines were set up to operate within tolerance.

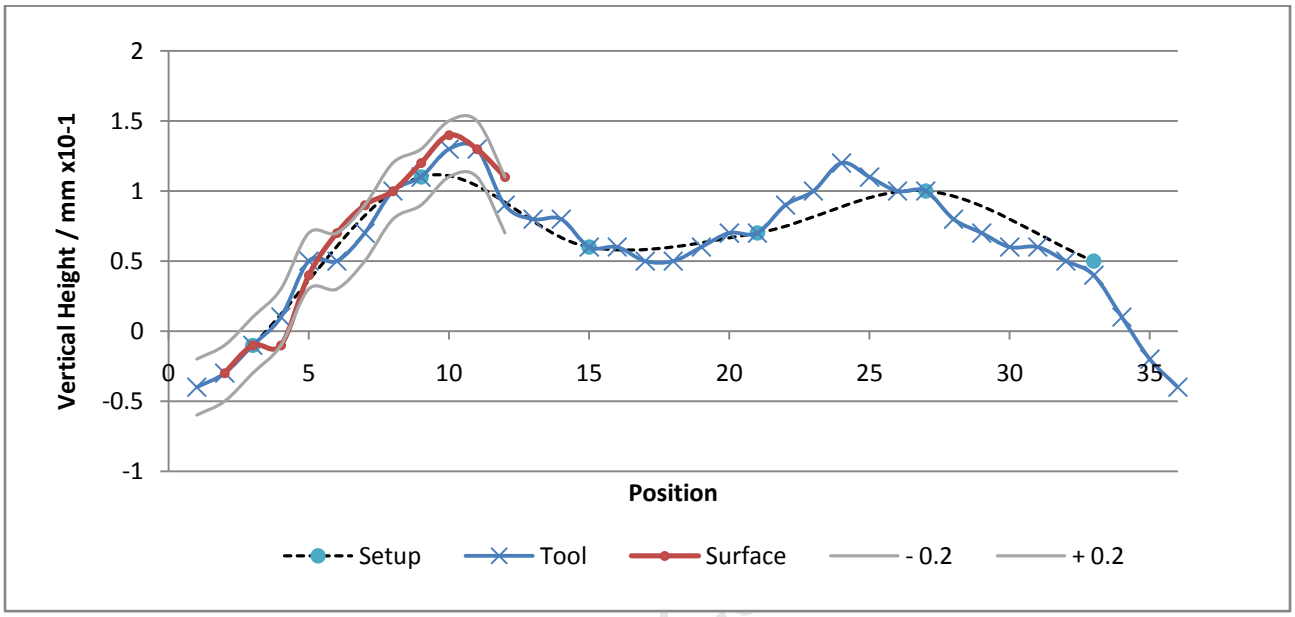

Figure 40: Test 1; M151.

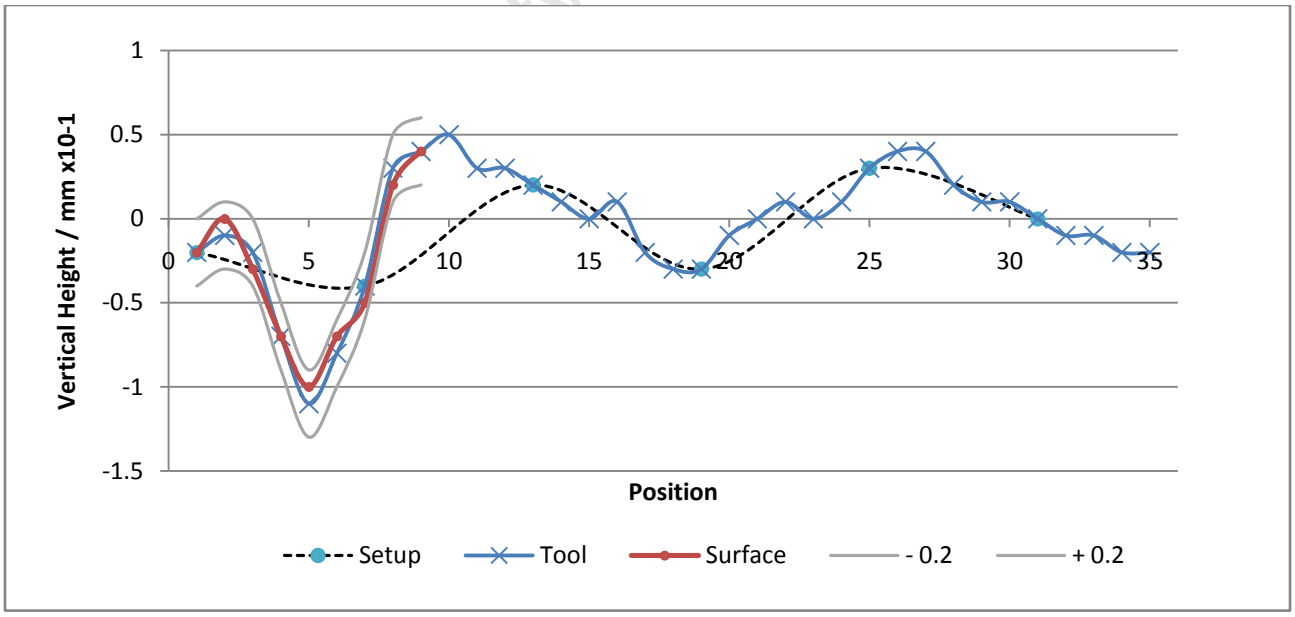

Figure 41: Test 1; M259.

4.4.3. Test 2 Results

The results illustrated in Figure 42 and Figure 43 were recorded from the second set of tests where the machines were set up to investigate the potential for a limit to the achievable performance.

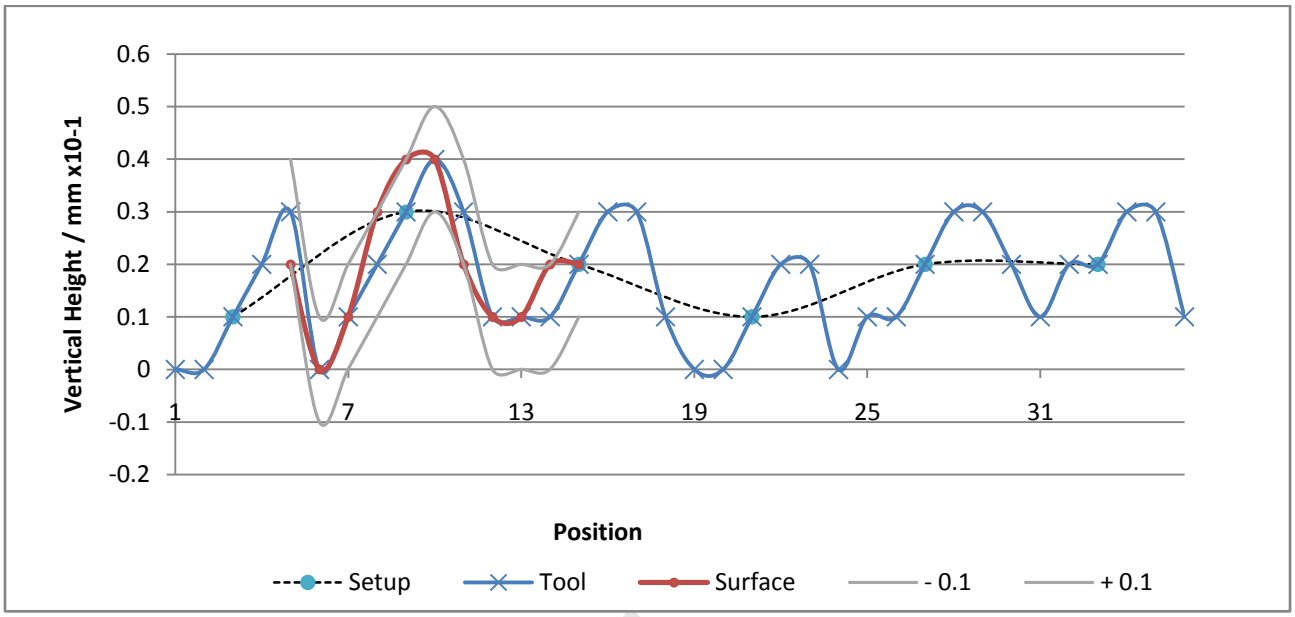

Figure 42: Test 2; M151.

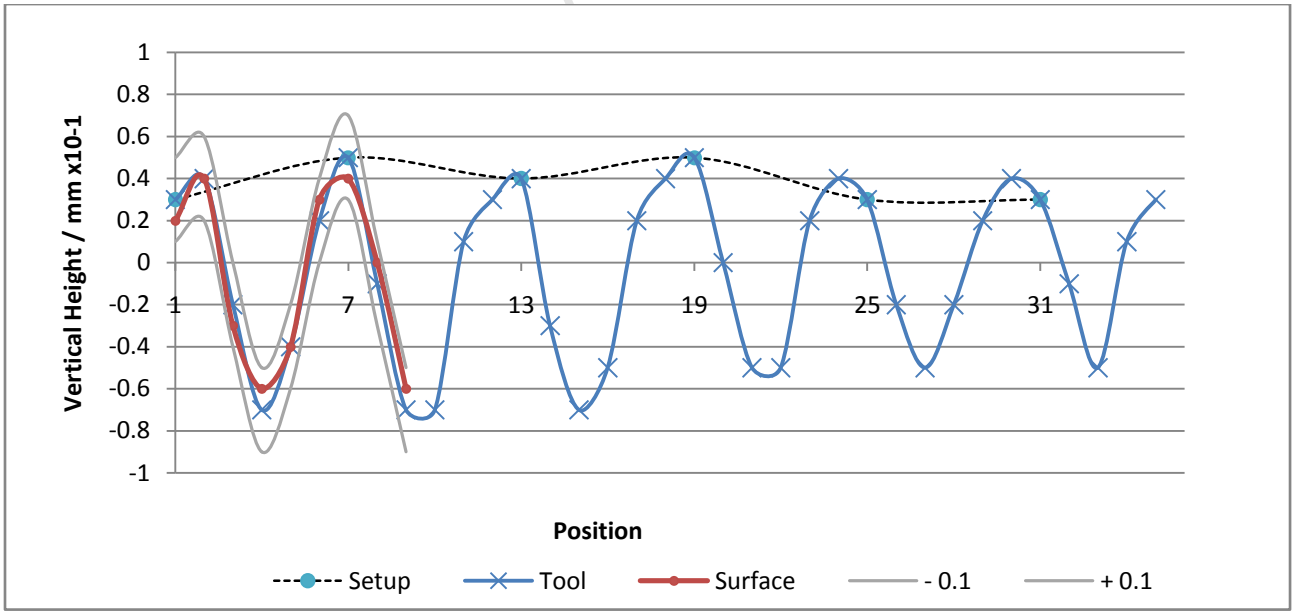

Figure 43: Test 2; M259.

4.5. Discussion of Milling Test Results

The objective of the two tests was to investigate the relationship between the engaged and the unengaged orbit, as well as to investigate the potential for a limit to the achievable performance. The results of which are discussed according to these two criteria. Figure 40 to Figure 43 illustrate the results of these tests as discussed below. In the results the lines labelled 'tool' represent the unengaged profile. The lines labelled 'surface' represent the profile measurement of the surface resulting from fully engaged milling. The 'setup' lines represent the points corresponding to each foot used for adjustment of the machine for un-flatness. For illustration purposes, the '-0.1', '+0.1' '-0.2', '+0.2' lines represent the uncertainty between the 'tool' and 'surface' plots.

4.5.1. Profile Correlation

The results from test 1 and test 2 could be used for assessing the correlation between the profiles.

Figure 40 and Figure 41 illustrate the direct correlation between the milled surface and the unengaged profile over the engaged section in test one. The uncertainty for both machines in the first test was +/–0.02mm. The machines in test 1 were set up to run within tolerance at the set diameter where the total un-flatness for the M151 in Figure 40 was found to be **0.17mm** and **0.16mm** with the M259 in Figure 41 respectively.

The second set of tests as illustrated in Figure 42 and Figure 43 respectively, were the results of the investigation into achievable accuracy. Notably, there is strong correlation between the two profiles. The uncertainty in the second set of tests was reduced to +/–0.01mm. While both tests reflect strong correlation between the unengaged and engaged profiles, the results of the second set of tests reflect a reduced uncertainty.

This uncertainty can be explained by the design used in both machines and the underlying path traversed by the tool in these tests. With the test for achievable accuracy the overall un-flatness is reduced and this in turn causes the arm to experience a smaller slope difference when rotating between the leg positions. On both machines the tool is offset from the centre of the arm relative to the X- axis.

This geometry will magnify the effects of the slope change experienced by the arm, as illustrated in Figure 44 below causing the tool to 'roll' about the X-axis. This suggests that the tool should be located central to the middle of the arm or that there should be a system in place to limit the induced roll.

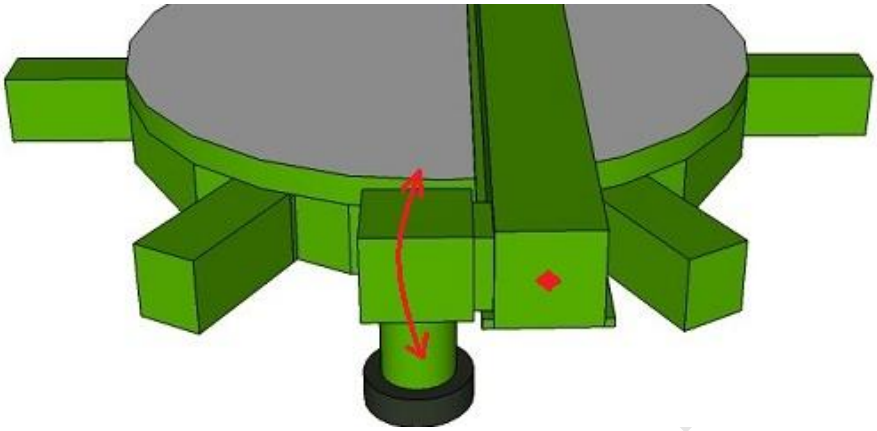

Figure 44: Illustration of offset tool.

4.5.2. Achievable Accuracy

In order to assess the achievable accuracy it was necessary to try to set up the machines to operate with an un-flatness as close to 0.00mm as possible, with respect to the points of adjustment around the orbit. This process not only assessed the performance of the machine but also tested the sensitivity of the feet that control the adjustment process.

M151

The results for the M151 are reflected in Figure 42. Here the six points corresponding to the feet were adjusted to be flat within 0.02mm. The total un-flatness attained was 0.04mm around the entire flange relative to the horizontal reference plane. On inspection of Figure 42 it is possible to see a cyclic pattern where the value rises and falls between each leg. The arm of the M151 lays offset from the middle of the base. At the setup points the tool is directly aligned with the closest foot. In this position the arm is partially over the intersection between the legs and the base. As the arm is rotated it is observable that the arm first rises as it traverses over

the supported section. This is followed by the value falling as the arm traverses the unsupported section.

This behaviour is comprehensible since the slewing bearing is designed to be coupled with supporting structures that provide structural rigidity, rather than the bearing being used as the structural element providing support. The achievable accuracy for the M151 was assessed by calculating the average difference in the rise and fall in each angular section. This isolates the 0.02mm un-flatness introduced in the setup and highlights the characteristic performance capability of the circular mill in question.

Achievable un-flatness	Φ3500mm
M151	**0.027mm**

The M151 uses feet illustrated in Figure 15 with two central set screws surrounded by four tensioning bolts. This was prone to introduce unpredictable results. By tightening the tensioning bolts in an unsymmetrical manner it was possible to introduce turning moments that affected the neighbouring measurements. This emphasised the need for a single point adjustment system on the feet that would not introduce unwanted forces.

M259

The results from the M259 illustrated in Figure 43 follow a similar pattern to those of the M151. On inspection it can be seen that again the arm traverses over a path that rises and falls in relation to the position of the arm to the legs. The design of the M259 differs from the M151 in that the arm is secured to the middle of the base.

The effect of this can be seen in the symmetry of the results. The high point corresponds to the adjustment point where the arm is above the leg-base intersection. The low point of the orbital path corresponded to the measurement points where the arm was resting on an unsupported section of the bearing. With the exception of the dimensional difference between the two machines, the position of the arm was the fundamental difference between the designs.

The achievable accuracy for the M259 was again determined by calculating the average un-flatness between each angular section. The setup un-flatness over the six adjustment points was 0.02mm. The calculated theoretical un-flatness is illustrated as follows.

Achievable un-flatness	Φ3500mm
M259	**0.099mm**

This result was counter intuitive since the larger M259 was designed for operating at larger diameters and appears to be a larger, 'sturdier' machine. It is suspected that this difference can be attributed to the centrally located arm. The arm weight on the M259 is larger than that of the M151 which could increase the 'sagging' effect between the legs.

4.5.3. External Influences

When testing with the DiNi 11 it was important to ensure that the operating conditions were suitable. The device was sensitive to environmental vibrations such as: a fork lift driving within a 10 meters radius, operation of the overhead cranes, heavy rainfall, high water level in the river nearby following heavy rainfall, and wind causing vibrations in the roofing structure. In on-site machining these are influences that are often present, which highlights the need to reduce the dependence on these highly sensitive equipment. Figure 45 illustrates the results of a measurement of a surface and orbital profile when two large vertical milling machines were operating combined with heavy rainfall. As per below, the two profiles reflect poor correlation with a maximum difference between the two of **0.25mm**. When a dial gauge was used to measure the relative change between the arm and surface, the maximum difference reflected 0.02mm between the tool and surface.

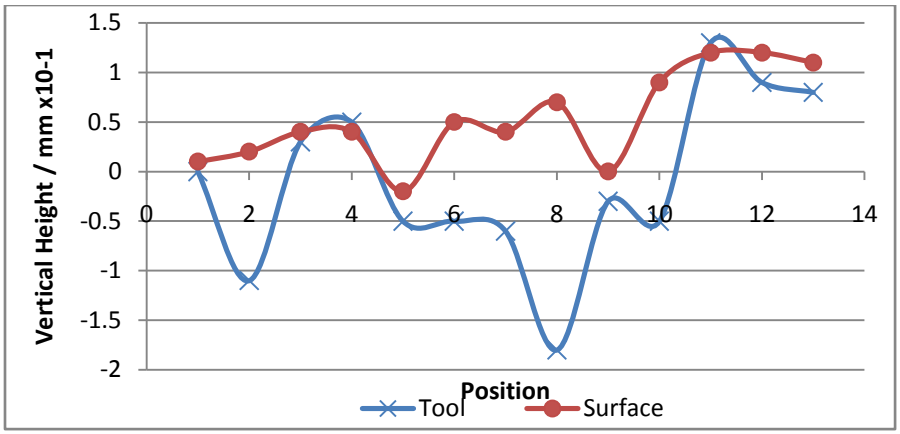

Figure 45: Measurements of the M151 effected by vibrations.

A further source of unpredictable results was due to the influence of sunlight. While the tests were performed within a hall with constant temperature, there were two semitransparent panels in the roofing that allowed sunlight to reach the machine. Sunlight from these panels caused the machine to deform in a non-linear, unpredictable fashion. The effect was most noticeable between the hours of 11am and 13pm when the sun was highest in the sky. When measurements were taken under these conditions, the measurements would change over time. It was possible that during the time required to measure 36 points around the orbit, the start/end point could vary by up to 0.3mm.

In order to counteract these influences, the milling tests were performed at night when the machine shop was inactive. The tests were all performed when there was no rain and the effects of the river were not apparent. This was achieved by repeatedly measuring the same point to ensure the measurement remained constant.

4.6. Comments on Existing Designs

4.6.1. Number of Legs

The two existing Wagner GmbH circular mills use 6 legs for mounting the machine. When the machine is first mounted and secured with three legs the initial adjustments are made with these three points. This rotates the machine about three axes. This system can be counter intuitive. The operators often use the dial gauge on the existing surface to measure four points that form a cross for adjustment.

This technique allows the adjustment to be performed about two axes. However, the use of 6 legs hinders the ability to effectively deploy this technique. It was also noted that the performance of the machine with the offset arm was superior to that of the symmetrically placed arm. This is because the arm remains in the region of the supported base for a larger section of the orbit.

Following on from this, it is proposed that by increasing the number of legs on the machine from 6 to 8 with the arms offset from the centre, the following can be achieved.

- Improved ease of use in the adjustment process by creating a system that supports a four point cross for adjustment.
- Improved achievable overall un-flatness in milling by reducing the angle between the legs and in turn increasing the number of supported zones around the orbit.

4.6.2. Internal Referencing System

The process of testing the M151 and M259 emphasised an area of poor performance within the referencing system. As discussed previously the precision measurement equipment is highly sensitive to vibrations. When the use of this equipment is prevented due to environmental conditions it becomes necessary that the operator uses the existing surface or another parallel surface to reference from. Often the existing surface is damaged or deformed, hence requiring machining. Alternatively there may be no suitable adjacent reference plane.

Currently under these conditions which are often met, it becomes difficult to operate these machines repeatedly within tolerance. It is desirable to have an internal referencing system that allows the following:

1. A referencing system that allows for the machine to be aligned so that that the cutting plane is within tolerance utilising the capabilities of the external referencing planes created by the electronic measurement devices.
2. A referencing system that allows the machine to be brought into tolerance without the use of the external measurement systems.

5. Design

5.1. Design Specifications

This project addresses the construction and design of a completely new circular milling machine. The project considers aspects of the design that are relevant to accuracy and repeatability, nevertheless it is important to outline the full set of requirements that were set out for the construction. The findings of this project and following design implementations were used in the construction of the circular mill. The Wagner GmbH Machine number for this circular milling machine was M391.

Geometric Requirements

- 500mm X-axis (radial) travel.
- 200mm Z-axis (axial) travel.
- Working diameter between ϕ2m and ϕ6m.

Physical Requirements

- Overall height less than 600mm.
- Two arms for securing the tool assembly.
- Use of the pre-purchased milling head.
- Use of the already purchased Rothe-Erde slewing bearing.
- Improved weight to operating diameter ratio.

Functional Requirements

- Design to be compatible with specified Siemens CNC hardware.
- Face milling and drilling.

5.2. Leg Interface and Internal Reference Plane

5.2.1. Remove Relative Measurement

Adjustment to the Wagner GmbH circular mills for parallelism has always been via the feet which rotates the base into orientation. Monitoring these adjustments has been achieved by measuring the movement of the upper machine relative to the work surface. As discussed before, errors on the existing flange can be introduced in the alignment process at this stage using this relative system.

Using the laser during the tests allowed for an absolute reference to measure from when adjusting for alignment, although this still presented the problem of adjusting the feet (below bearing) while measuring the tools position (above bearing). As a result the adjustment process was not easily predicted resulting in a more time consuming procedure with the potential to introduce errors due to the existing flange profile.

While the use of the external referencing systems does eliminate the error introduced by relative measurement, these cannot always be used. Under the influence of environmental vibrations the function of these devices can be limited causing reduced precision or even preventing the use completely.

It became apparent from the testing of these machines that knowing the position of the legs in space would be beneficial. Adjustment of the feet controls the alignment of the bearing as well as the flatness of the surface it lies on. The flatness resulting from adjustment of the feet in turn controls the un-flatness in the final milled surface. In order to monitor the position of the legs it was important that the design of the interface allow locational repeatability when reassembled and reconfigured to different mounting diameters.

In previous designs used by Wagner GmbH, there has been no complete locational accuracy in the mounting of the legs relative to the base as well as the legs to the feet. This in turn made it impossible to measure the positions of the legs relative to each other or to use the legs as a reference in the setup of the machine. Being able to measure the positions of the legs allows for an understanding of the surface that the bearing rests on to be attained, provided that the interconnecting components are designed and manufactured to facilitate this.

The principle with the leg interface system was to control the manufacturing process in such a manner that a reference plane could be created with a controlled uncertainty between the position of the reference and the bearing. This meant using functional dimensioning that would reduce tolerance stacking in the assembly. Since each leg section used is made from the same raw material and manufactured in the same manner, it is assumed that each section will respond to the forces produced by adjustment and deflect in a similar manner to the others. It follows that along with ensuring repeatability within the interface system there should be a controlled surface from which measurements are made.

5.2.2. Design

Bottom Base

The commissioning of M391 circular milling machine, allowed the freedom to design a complete system that would facilitate a new measurement and adjustment process and in turn improve the control over the primary profile produced by the machine.

Figure 46 below illustrates the components of the circular mill that mount below the bearing and form the alignment system. This system is comprises of the bearing (1) which is secured to the bearing flange (2). The octagonal hub (3) and base legs (4) amass the bottom base assembly which mount to the lower surface of the bearing flange. The legs (5) are secured to the bottom base using the interface discussed herein. The feet (6) use this same interface to mount to the legs or bottom base. This assembly constitutes the lower half of the machine. Onto the upper surface of the bearing mounts the top plate, arms with extensions, tool and counterweight. The machining processes used in constructing the bottom base were controlled to ensure the designed tolerances were met as this subassembly serves as the foundation to

the new alignment system. It was essential that the tolerances were met to avoid unwanted stacking of out of tolerance errors. These dimensions and tolerances are discussed in the following text.

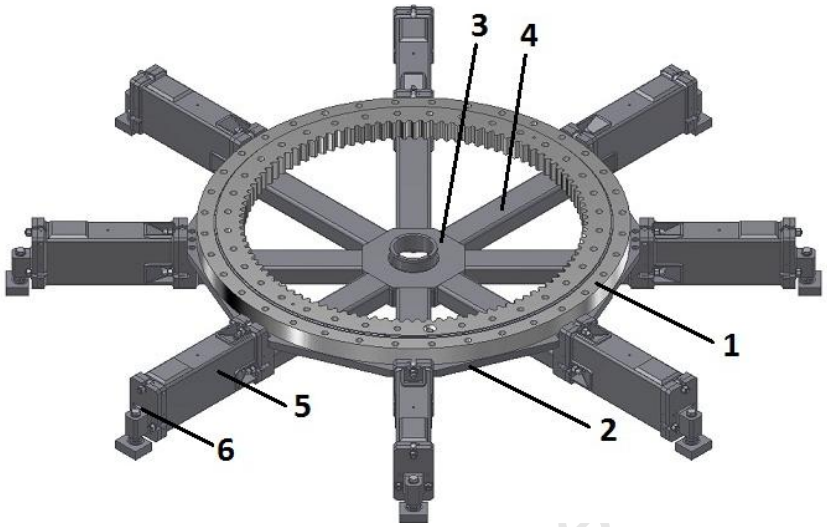

Figure 46: Alignment system and bearing.

Interface System

The interface system was introduced to ensure that the base legs, legs and feet have locational certainty each time they are assembled. This would allow the bottom base to be used as a locational reference. The interface between the legs, base legs and feet can be viewed in Figure 47. In the manufacturing process, the surfaces labelled (1) were used as the reference for all dimensioning. For locational repeatability, two DIN EN ISO 2338 ϕ10mm h8 dowel pins were used. These pins combined with the mating surface between each component resulted in movement within the interface being restricted in all three translational directions as well as rotational axes. The dimension (X) between the reference surface and the dowel pins being 110 mm $^{+}/_{-}$0.01mm, the holes were drilled and reamed on a rotatable milling bed, allowing the holes to be at the same dimension relative to the reference surface on either end of the arm. The position of surface (3) relative to the reference was tolerance with the same $^{+}/_{-}$0.01mm. By using the surfaces labelled (1) as reference for the interface, it was possible to rest the arms on the table of the milling bed using this surface. This helped to ensure that the $^{+}/_{-}$0.01mm tolerance was met.

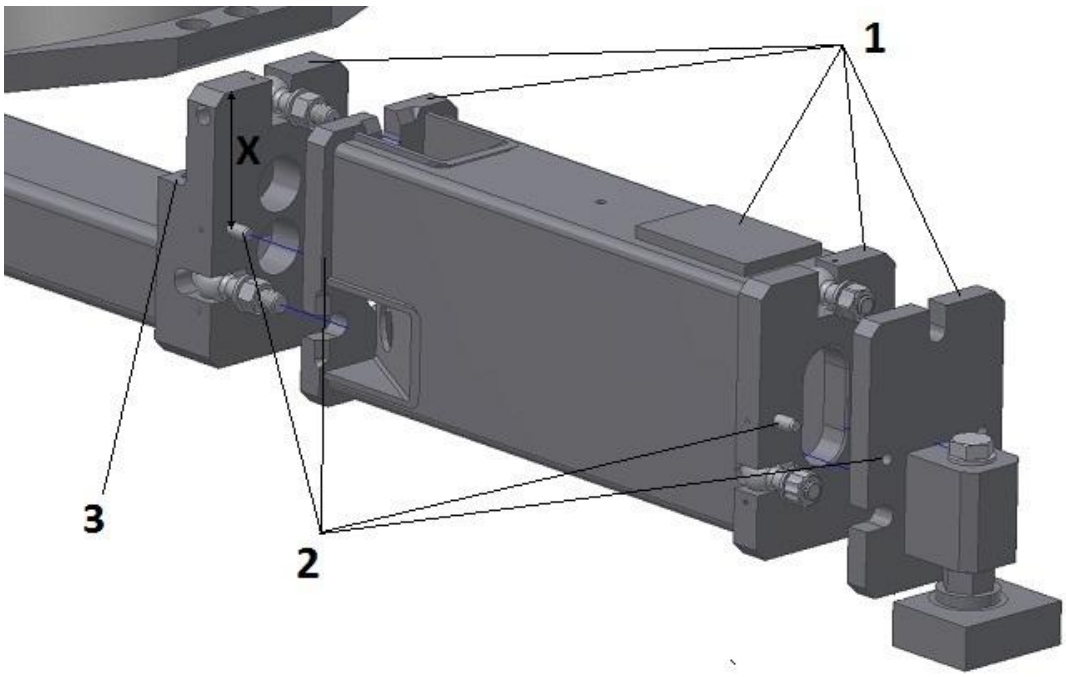

Figure 47: Separated base leg, leg and foot.

By using combinations of legs, the diameter that the feet are mounted at is adjusted. The maximum diameter for mounting uses a combination of 4 legs joined to the base leg and foot. As illustrated in Figure 47, each leg has an uncertainty of $^{+}/_{-}$0.01mm in the z direction of the dimension X between the reference surface and dowel pins. As well as the base leg which has the extra dimension to surface (3) also toleranced to $^{+}/_{-}$0.01mm. The thickness of the flange is turned to be within a tolerance of $^{+}/_{-}$0.02mm around the surface. This is combined to result in a maximum uncertainty between the position of the outermost reference surface at the maximum diameter (ϕ6660mm) and the lower bearing surface is:

$$(^{+}/_{-}0.01\text{mm}) \times 6 + (^{+}/_{-}0.02\text{mm}) = ^{+}/_{-}0.08\text{mm}$$

When assembled these surfaces combine to form planar reference rings. A 120mm x 80mm plate is welded to the upper surface of the rectangular tube which is large enough for the magnetic bases from the levelling device and other digital lasers. Figure 48 illustrates the rings formed by the reference surface at different diameters.

Figure 48: Bottom base with emphasised referencing surfaces.

Feet

Once secured to the work, the bottom base is adjusted for alignment using the feet. The new design for the feet addressed some of the issues found in the current feet. With the M259 feet there was an improvement in the predictability of adjustment of the aforementioned feet over that of the M151. Since the focus was on a single point of adjustment with the tensioning bolts around this there were minimal induced rotations moment that would effect the measurements of the adjacent positions.

In order to try to eliminate the induced forces and simplify the adjustment process, the following design was proposed. As illustrated in Figure 49 the adjustment is made by an M45x1.5mm adjustment screw (1). The mating surface between the screw (1) and welding plate (2) has a radius of 200mm. This ensures that when the height of the foot is adjusted that there is always full contact between two components. This pivoting joint also prevents induced forces from the adjustment process.

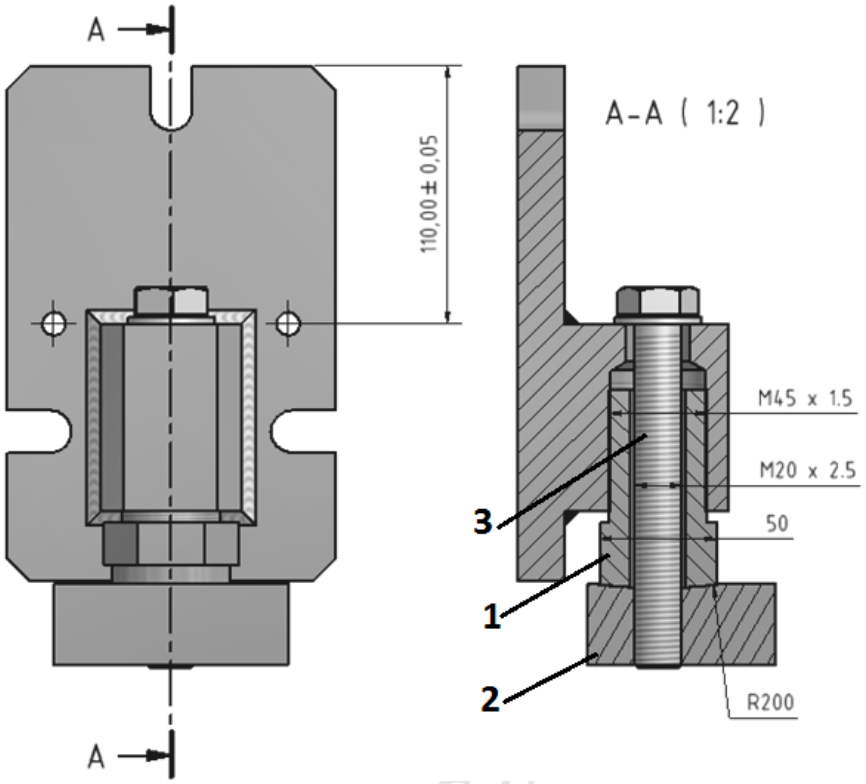

Figure 49: M391 foot.

A problem encountered with the current feet was that adjustment of the tensioning bolts had an effect on the tool path. This was due to the set screws and tensioning bolts adjusting the same plate of metal that could alter the position of the leg. In order to reduce this effect, the tensioning bolt is concentric with the adjustment screw. The mating surface between the base of the foot and the bolt being above the contact zone in the thread. When the tensioning bolt is fastened the deformation in the base does not effect the position of the foot.

The same 110 $^{+}/_{-}$0.05mm reference was used for the locating H7 holes on the feet. Although the reference surface of the feet is not used in the measurement process.

5.3. Cassette

The objective of the cassette design was to address the lack of control over tool orientation in the1st and 2nd generation circular milling machines. Tool orientation during the milling process has a direct control over the resulting surface lay. A poorly oriented tool will produce an anisotropic surface due to the insert geometry and combined feed velocity. The tool orientation can also introduce taper errors in the outcome surface when the inner and outer inserts of the tool relative to the machine are not horizontally level. As stated previously, the modern slewing bearings require mating surfaces that have controlled profiles as well as taper errors. The design features detailed below address the issue of tool orientation control with a focus on ease of use in attaining an accurate and repeatable orientation.

Pitch Control

In both the Wagner GmbH M151 and M259 circular milling machines, the milling head assembly housed the mechanics for both the X axis movement and the Z axis. In the M391 machine the X axis movement is attained by movement of the entire arm assembly relative to the base of the machine. This alteration allows for the milling head assembly, (illustrated in Figure 50) to house the mechanics for only the Z-axis movement as opposed to the X and Z as in the M151 and M259..

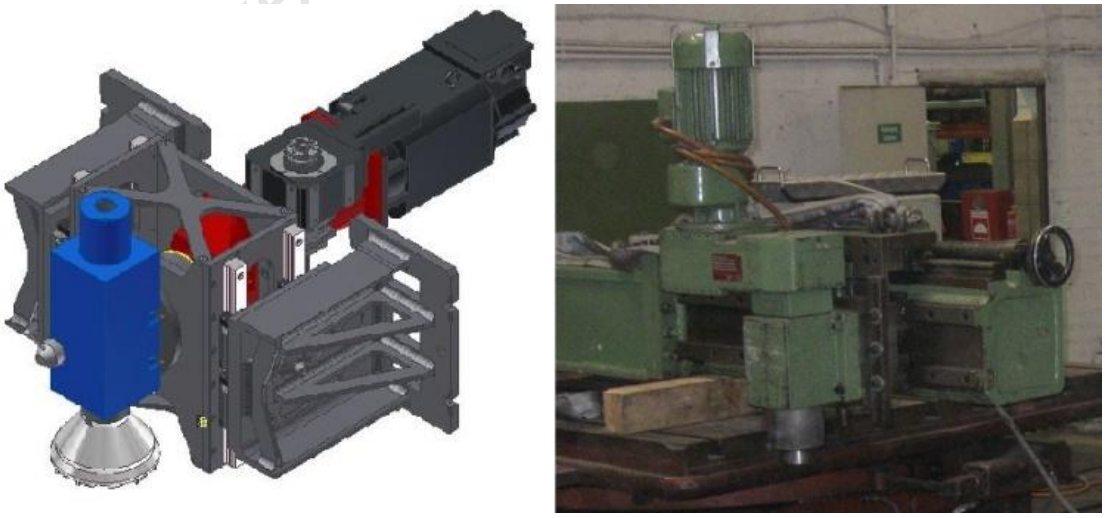

Figure 50: M391 and M151 milling head assemblies.

By separating the assembly in this manner it becomes possible to isolate the mechanics so that that the milling motor, gearbox, components for Z-axis movement, milling head and tool can be isolated in a single subassembly. De-coupling the components in such a manner allows the interface between the cassette and arm end to be used as a pivoting point for the cassette sub assembly.

Figure 51 illustrates the cassette isolated in the left image. The right image in Figure 51 illustrates the sectioned cassette joined to the left arm end by a pin, emphasised by the red circle through both the cassette and arm end. This feature is repeated symmetrically on the cassette allowing the assembly to “pitch” about the cc-axis. Three M12 screws are used per side to secure the cassette orientation as well as a single M16 screw that secures to the pitching pin. The pitch adjustment allows for the user to adjust the tool to correct taper errors. The three M12 bolts are secured in circular slots that allow $\pm 5°$ rotation of the tool from level operation.

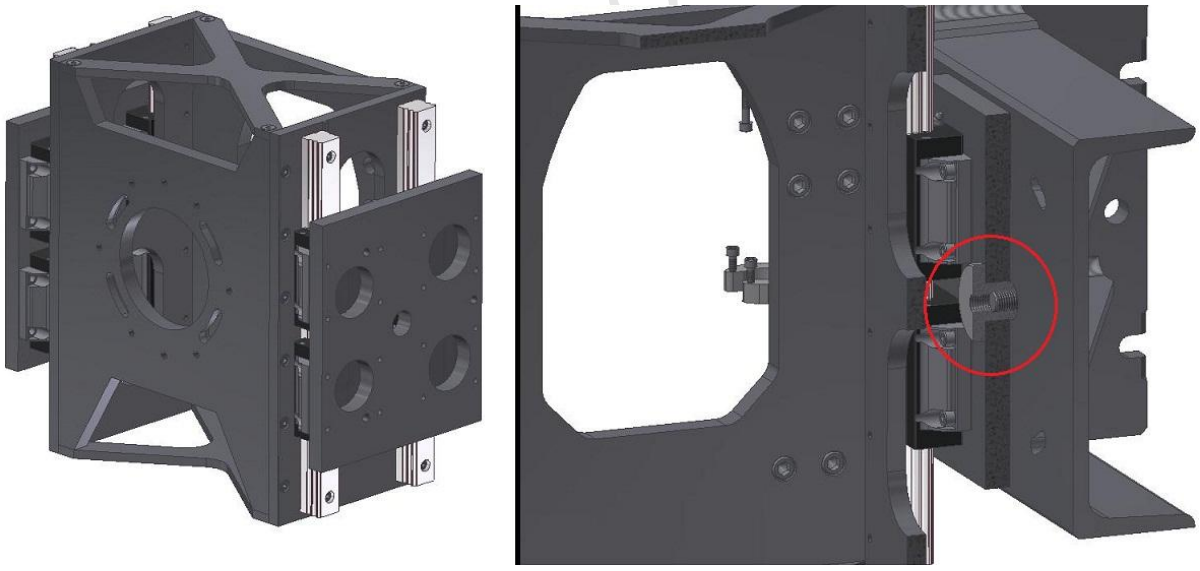

Figure 51: Cassette entailing pitch features.

Roll Control

Poor tool orientation causes the tool to leave an undesirable surface topography. This manifests in the form of anisotropic lay. The characteristic lay marks produced in circular milling are illustrated in Figure 52. They are formed when the leading or trailing inserts (illustrated in Figure 52) of the misaligned tool are not on the same plane relative to the cutting plane. When the tool is misaligned in such a manner, the geometry of the tool creates a concave surface which in effect is a taper error and effects the total un-flatness.

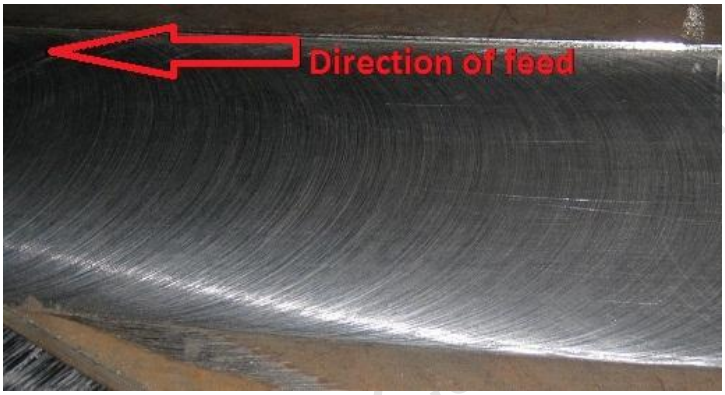

Figure 52: Anisotropic lay due do misaligned tool.

In the M151 and M259 the tool assembly was secured to the arm with no adjustment possible for aligning the tool to the surface when misaligned. Adjustment was often attained by inserting metal shims in the interface between components that would allow the tool to rotate the direction required to align the tool to the required surface. The lay produced in Figure 52 was induced by inserting shims that caused the trailing inserts to be horizontally lower than the leading inserts.

This technique is time consuming and at times may require the use of a crane to lift the milling head assembly in order to create the necessary space for inserting the shims. The efficacy of the shims was also effected by the amount of preload used in tensioning bolts that secure the milling head assembly.

The poor functionality of the existing milling head system brought to light the need for the M391 to be easily adjustable in the 'roll' direction. Ensuring that the tool is always perfectly aligned to the surface results in:

- improved surface topology, and
- reduced un-flatness due to geometric effects of the misaligned tool.

Figure 53 below illustrates the milling head and cassette where the milling head is de-coupled. In this figure the two highlighted cylindrical surfaces represent the interface that permits the 'roll' functionality in the milling head. The cylindrical surface on the milling head had a dimension of ϕ139.95 which corresponded to an f7 tolerance. This allowed the mating surface to be dimensioned to ϕ140 H7 which produced a clearance fit, enabling the components to be easily assembled and the ability to rotate by hand when the fastening bolts are not secure. When the fastening bolts are secured the milling head is secured and unable to rotate.

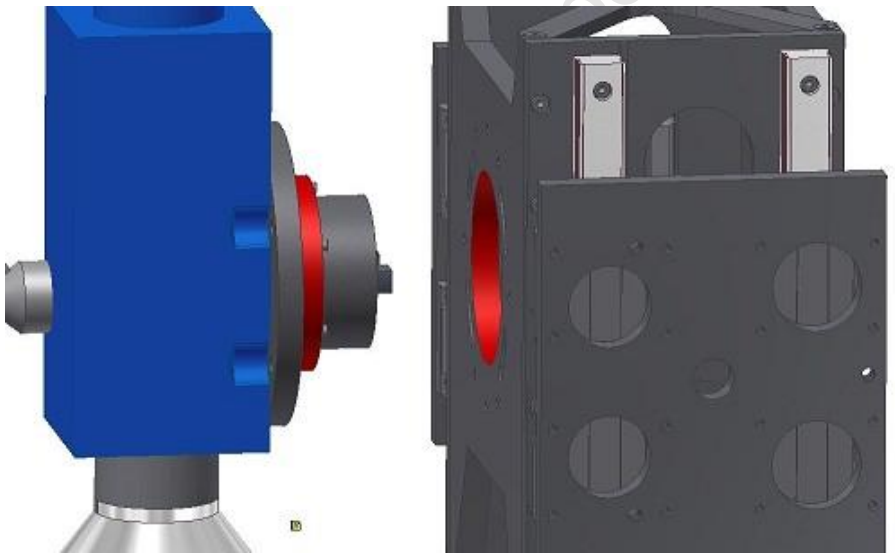

Figure 53: Cassette and milling head coupling interface.

In order to secure the milling head in the variable positions when rotated, the holes for the securing bolts between the two components were milled into slots. These slots allowed $^{+}/_{-}13°$ of adjustment. This adjustment allowed the tool orientation to be controlled by loosening the bolts and rotating the head without the need for an overhead crane or shims. The system also allowed the milling head to be rotated about 180° enabling overhead milling.

5.4. Arms

5.4.1. Outline of Arm Function

The function of the arm assembly is to connect the core of the machine and the machine tool assembly. In doing this the arm length and position also contributes to the determining of the operating diameter. The arm assembly is separated into 3 separate component groups with individual functions described below:

- The arm: Attaches the arm to the upper plate of the machine.
- The arm extension: Placed between the arm and arm end. Combinations of these determine the operating diameter
- The arm end: The cassette and tool attach to this.

The separation of the components enables the optimum arm length to be chosen that matches the work diameter. This prevents the machine from being transported at an excess, unnecessary weight, in turn saving transportation costs.

In order to improve the performance of the current machines, it is necessary to have a quantitative method of comparison. The student edition of Autodesk Inventor 2010 has an integrated FEM simulator. The performance of the profiles was evaluated in 2 simulations measuring displacement relative to various forces that would simulate the operating conditions. Each profile tested was the same length, 1meter and subjected to the same simulation conditions. Below are descriptions of each test followed by tabulated results.

5.4.2. Two Arm Design

One of the design requirements was to use two arms to connect the base and the milling head assembly. While this was a requirement, the findings of this project have emphasised that the use of two arms could improve the performance of the M391 machine by achieving the following:

- Securing the milling head from two sides and preventing the ‘roll’ effect discussed in 4.5.1.
- Two offset arms providing four points of contact with the bearing around the base circumference.

5.4.3. Simulation 1

The objective of the first test was to determine the most effective cross section profile for the Arm assembly. The results thereof would be used to compare to the current profiles. Each profile selected had 200mm height with exception of the U profile which was 300mm in height. The thicknesses selected were such that their mass per unit length was between 45kg and 50kg.

Simulation 1 Forces

The forces used in the first simulation were arbitrary values that roughly matched those produced by the cutting process and the cassette weight.

Fz = 5000N

Fx = 1500N

Mx = 505.5 Nm

Fcc = 650N at distance from centre 337mm Xo from Linear bearing calculation

Mcc = 219.05 Nm

Simulation 1a: Horizontal

Force of 5000N applied to the non fixed end of the cantilever. The direction of the force and gravity were both downwards in the negative z direction. This assesses the ability of each profile to resist deflection in the direction of the thrust component of the cutting force (δz) while the machine is operating in a plane parallel to the horizon.

Simulation 1b: Vertical

In this simulation a single force of 5000N is applied to the non fixed end of the cantilever parallel to the z-axis of the machine. Gravity is perpendicular to the z-axis and the arm is parallel to the horizon, this simulates the forces acting on the cantilever if the machine were in a vertical operating position. Deflection in both the cc and z directions were measured

Simulation 1c: Complete

In the complete simulation, forces in three axes are considered: The thrust force in the z-axis as well as moments created by the forces in the tangential and radial directions. Deflections are measured in directions parallel to the cc and z axes.

Results of Simulation 1:

			1a: Horizontal	1b: Vertical		1c: Complete	
		kg/m	δz / mm	δz / mm	δcc / mm	δz / mm	δcc / mm
DIN 10210	200x200x8mm	47.3	0.265	0.254	0.011	0.297	0.0167
DIN 10210	200x120x10mm	45.6	0.315	0.303	0.0227	0.355	0.0412
DIN 10056	200x150x15mm	47.1	0.569	0.558	0.496	0.669	0.6111
DIN 10056	200x200x16mm	48.2	0.737	0.567	0.362	0.677	0.4384
DIN 1026	U-300	46.2	0.54	0.229	0.533	0.253	0.5994

Table 8: Simulation 1 results.

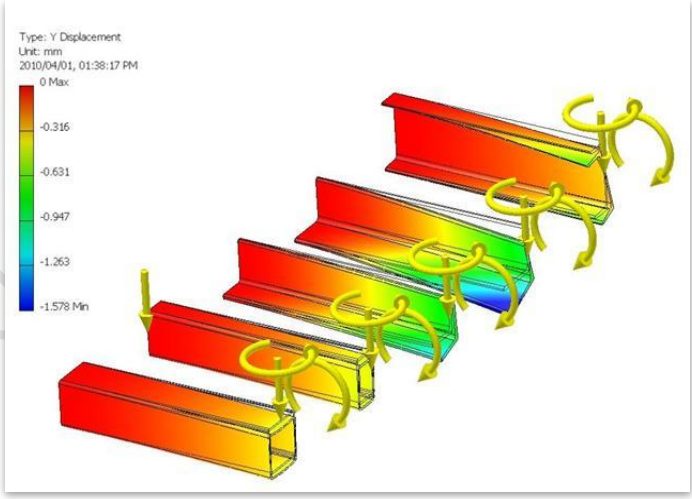

Figure 54: Components of simulation 1c.

5.4.4. Discussion of Arm Simulation 1

1a: Horizontal Performance

The top two performers were the rectangle and square DIN 10210 profiles. Both DIN 10210 profiles outperformed the L and U profiles by a margin of at least 40 percent. Between the rectangle and square profile, the square profile deflection in z-axis was 15% improved. Even though the height of the U profile was 100 mm larger, the performance was still poor. This could be attributed to the unsymmetrical shape causing twisting under load. Both the L and U profiles showed the natural inclination to twist under load, as reflected in Figure 54.

1b: Vertical Performance

In the vertical simulation, the z direction results were similar to those of the horizontal simulation. In the z direction, the U profile performance was significantly increased from −0.54mm to -0.229mm although performance in the cc direction was the poorest. With the exception of the U profile, the cc axis results highlighted the square and rectangular profiles as being superior.

1c: Complete

In the complete simulation the two best performers were again the square and rectangular profiles, in both directions. In the z axis the U profile performed well, although the deflection in the cc direction was poor and negates this.

From the results achieved it is evident that the unsymmetrical L and U profiles reflect a natural tendency to twist. When the thrust force and gravity are perpendicular, the profiles deflection in one of the directions may be satisfactory, although this is typically accompanied by poor performance in the perpendicular direction. This inconsistent behaviour is therefore not desirable.

The two symmetrical profiles consistently performed well. In the vertical test the square profile was significantly superior. Looking at the equation for "I" and the corresponding Izz values for the two profiles, this is understandable since there is a 60mm difference in height which would be cubed and therefore have a profound effect. From these results, it was concluded that in the second set of simulations, various DIN 10210 profiles should be tested against the current Wagner GmbH profiles in order to evaluate performance and identify the optimum configuration.

5.4.5. Simulation 2

Following on from the findings in simulation one, simulation two investigated the performance of various DIN 10210 square and rectangle profiles with an aim to identify the optimum profile for use in the arms. The selected sizes had variable heights between 200 mm and 450mm and widths between 200mm and 400mm. Each profile selected was simulated in 4 wall thicknesses, 16mm, 12.5mm, 10mm and 8mm.

In this set of simulations, the forces used varied from the first test. The M391 machine would use two arms instead of the current single arm setup. Based on this, the assumption that each arm would bear 50% of each load was made and therefore the forces applied to the DIN 10210 profiles was half of those applied to the current Wagner GmbH profiles.

In the second set of simulations, the deflection due to gravity and the cutting forces were separated into three simulations. Two of the tests were focussed on the beams bending under their own weight and one test showing the effects of the cutting force acting on the end of the beams. It was possible to separate the tests accordingly, as the direction of the cutting force relative to the co-ordinate system of the machine remains constant relative to the machine, whereas gravity changes direction depending on the working setup of the machine.

5.4.6. Cutting Forces

The force calculations were based on the following cutting conditions with a 200mm face milling tool. The material used was 42CrMo4 since it is the toughest material encountered by the circular mills.

Feed rate

$$v_f = f_t \times T \times n$$

$$v_f = 0.1 \times 11 \times 279$$

$$v_f = 306.4\text{mm/min}$$

Chip thickness

$$h \approx 0.9 \times f_t$$

$$h \approx 0.09\text{mm}$$

Pressure angle

$$\sin\left(\frac{\phi s}{2}\right) = \frac{a_e}{D}$$

$$\phi s = 2 \times \sin^{-1}\left(\frac{a_e}{D}\right)$$

$$\phi s = 2 \times \sin^{-1}\left(\frac{0.2}{0.2}\right)$$

$$\phi s = 180°$$

Effective Teeth

$$T_e = \frac{\phi s \times T}{360°}$$

$$T_e = \frac{180 \times 11}{360°}$$

$$T_e = 5.5$$

Chip section

a_p	Cutting depth in mm	1.25 mm
a_e	Engagement (milling width) in mm	200mm
v_c	Cutting speed in m/min	175m/min
n	Rotational speed in rpm	279rpm
D	Cutting diameter in mm	200mm
T	Number of teeth	11
F	Feed per revolution in mm	0.1mm
f_t	Feed per tooth in mm	0.1mm

Table 9: Cutting data.

F_c	Cutting force in N
A	Chip section in mm^2
k_c	Specific cutting force in N/mm^2
a_p	Cutting depth in mm
a_e	Engagement (milling width) in mm
v_c	Cutting speed in m/min
v_f	Feed rate in mm/min
n	Rotational speed in rpm
D	Cutting diameter in mm
T	Number of teeth
F	Feed per revolution in mm
f_t	Feed per tooth in mm
h	Chip thickness in mm
T_e	Effective no of engaged teeth
ϕ_s	Active cutting angle

Table 10: Constants for calculating Fc.

$A = a_p \times h \times T_e$

$A = 2 \times 0.09 \times 5.5$

$A = 0.18\text{mm}^2$

Cutting force

$F_c = A \times k_c$

$k_c = 2280\ N/mm^2$ was selected from a table where

$F_c = 256.5$ N per engaged tooth

Shear angle for calculated tool used in k_c table.

$$\emptyset = \frac{5}{8}\alpha + \frac{1}{2}\text{acos}\left[e^{\left(-52.5\times10^3\left(\frac{\sigma_u}{100\rho c}\right)^{0.8}\left(va\times\frac{10^3}{\omega 60}\right)^{0.4}\right)}\right]$$

$\emptyset = 29.42°$

Calculate friction angle.

$\eta = \lambda$

$\eta = 17°$

$\emptyset = 45 - 0.5(\beta - \alpha) - 0.5\beta$

$\beta = 24.08°$

Calculation of k×a×b.

$$F_c = k \times a \times b \times \frac{[\cos(\beta - \alpha)\cos\lambda + \sin\beta \sin\lambda \tan\eta]}{\sin\emptyset\cos(\emptyset + \beta - \alpha)}$$

$k \times a \times b = 90.2$ N

σ_u	Ultimate tensile stress	1300Mpa
ρc	Density x specific heat	3.91 x 10^6J/m^3
α	Effective rake (radial)	6°
ω	Thermal conductivity	1.42x10^{-5} m^2/s
a	Chip thickness	0.1mm
v	Cutting velocity	185 m/s
λ	Inclination angle	17°

Table 11: Values for first shear calculation.

Shear angle for actual tool.

$$\emptyset = \frac{5}{8}\alpha + \frac{1}{2}\text{acos}\left[e^{\left(-52.5\times10^{3}\left(\frac{\sigma_u}{100\rho c}\right)^{0.8}\left(va\times\frac{10^{3}}{\omega 60}\right)^{0.4}\right)}\right]$$

$\emptyset = 25.67°$

Actual friction angle.

$\eta = \lambda$

$\eta = 17°$

$\emptyset = 45 - 0.5(\beta - \alpha) - 0.5\beta$

$\beta = 27.83°$

σ_u	Ultimate tensile stress	1300Mpa
ρc	Density x specific heat	3.91 x 10^6J/m^3
α	Effective rake (radial)	6°
ω	Thermal conductivity	1.42x10^{-5} m^2/s
a	Chip thickness	0.1mm
v	Cutting velocity	185 m/s
λ	Inclination angle	17°

Table 12: Values from actual shear calculation.

Calculate force components

$$F_c = k \times a \times b \times \frac{[\cos(\beta - \alpha)\cos\lambda + \sin\beta\sin\lambda\tan\eta]}{\sin\emptyset\cos(\emptyset + \beta - \alpha)}$$

$$F_r = k \times a \times b \times \frac{\sin(\beta - \alpha)}{\sin\emptyset\cos(\emptyset + \beta - \alpha)}$$

$$F_a = k \times a \times b \times \frac{[\cos(\beta - \alpha)\sin\lambda - \sin\beta\cos\lambda\tan\eta]}{\sin\phi\cos(\emptyset + \beta - \alpha)}$$

$F_c = 310.04$ N Parallel to insert velocity

$F_r = 163.10$ N Towards centre of rotation of tool

$F_a = 42.64$ N Parallel to axis of rotation of tool.

Resolve according to machine coordinate system

$F_{cc} = \sum(F_c\cos\theta_i - F_r\sin\theta_i)$ Where $\theta_i = (n-1)\frac{360}{T}$

$$F_x = \sum(F_c\sin\theta_i - F_r\cos\theta_i)$$

$$F_z = \sum(F_a)$$

Tooth	Engagement	Angle	Fcc	Fx	Fz
1	1	0.0	310.0	163.1	42.6
2	1	32.7	172.6	304.8	42.6
3	1	65.5	-19.6	349.8	42.6
4	1	98.2	-205.6	283.7	42.6
5	1	130.9	-326.3	127.5	42.6
6	1	163.6	-343.4	-69.1	42.6
7	0	196.4	0.0	0.0	0.0
8	0	229.0	0.0	0.0	0.0
9	0	261.8	0.0	0.0	0.0
10	0	294.5	0.0	0.0	0.0
11	0	327.3	0.0	0.0	0.0
		Σ	**-412.2**	**1159.7**	**255.9**

Table 13: Forces resolved to machine coordinate system.

$F_{cc} = 412.2\ N$

$F_{x} = 1129.7\ N$

$F_{z} = 255.9\ N$

2a: Gravity

These simulations represent the static deflection that is present due to gravity. The two gravity tests demonstrate the deflection in the beams due to gravity in two directions. "horizontal" is when gravity acts in the direction that it would be when the machine operates in a plane parallel to the horizon. Deflection in this mode is termed δz and is parallel to the z-axis of the machine. "Vertical" is where the machine is operating in a plane perpendicular to the horizon, i.e. vertically. The deflection in this mode is termed δcc and is parallel to the circumferential cutting force or cc-axis.

2b: Cutting Force

This simulation involved the cutting forces from the tool applied directly to the end of the beams, excluding the static deflection from the effect of gravity. The geometry of the cutting tool and arm end assemblies that would introduce further bending moments was excluded since the geometry in the existing Wagner GmbH machines and the M391 were not similar, providing a more comparative set of results. The cutting force was resolved into three components in the z, x and cc directions. Deflections were measured in two directions parallel to the z and cc axes.

Discussion of Results

The force simulation demonstrated the profiles' ability to resist deformation due to the cutting force. A few trends are noticeable in these simulation results. On inspection of the bending characteristics, the height (in direction of measured deflection) is inversely proportional to the deflection. This can be viewed in Figure 57 comparing the 250x250, 350x250 and 400x250 profiles in δz deflection as well as the δcc in Figure 58. All three profiles have the same width and varying heights - the smallest height producing the largest deflection and the largest profile producing the smallest deflection. These results showing that a taller profile is more able to resist deflection. There is also a noticeable correlation between the wall thickness and deflection. Following on from this, each set of profiles demonstrated that larger wall thicknesses are more able to resist deflection due to force.

The gravity tests demonstrated the profiles ability to resist deflection under its own weight. The one trend noticed in the results from these simulations was similar to the force tests in that the profiles with larger heights had superior performance over the smaller profiles, which can be observed in Figure 55. The second, less intuitive trend was that the profiles with larger wall thicknesses produced larger deflections due to gravity as observed in Figure 55 and Figure 56. This is understandable since the larger wall thickness produces a larger distributed mass (illustrated in Figure 59) which in turn produces a larger distributed force due to gravity and in turn a larger deflection.

The mass of the cassette was not included in the simulations. It would produce a static force acting parallel to gravity and the results of the force test are sufficient to demonstrate each profiles ability to resist deflection due forced applied at the end of the cantilever. This can be observed from the formula below for the deflection in a cantilevered beam where deflection, δ is proportional to the applied force, F.

$$\delta = \frac{F \times l^3}{3 \times E \times I}$$

The purpose of this section was to identify the optimum profile to be used in the dual arm setup of the M391 machine. It is worth noting that in each test, the results for the M151 and M259 were included for comparison. The M151 machine has a maximum stable operating diameter of ϕ5m and the M259 operating at a maximum of ϕ9m, with the M391 operating at a maximum of ϕ 6.5m. One of the main design constraints for the M391 was to keep the overall weight as low as possible.

The results from the static gravity tests reflected that the larger wall thicknesses produced more static deflection. The larger wall thickness represents excess mass. This was contrasted by the trend in the cutting force tests, where the larger wall thickness produced less deflection.

Because the bending moment ($M = F \times l$) is largest at the base of a cantilever, it follows that the wall thickness should be larger closer to the base of the arms and can be thinner towards the free end. By tapering the wall thickness in this manner, it reduces the overall mass of each arm section, while reducing the deflection due to gravity. By using a tapered wall thickness setup in this manner, it allows for the selection of final profile to be done comparing each profile series rather than individual tubes and wall thickness combinations.

The selected series was the rectangular, 350x250 DIN 10210 series in the tapered setup. The results of the force tests illustrate that the M391 performance was similar to that of the un-tapered 350x250x16mm profile while being 16.4% lighter when comparing the M391 to the M259.

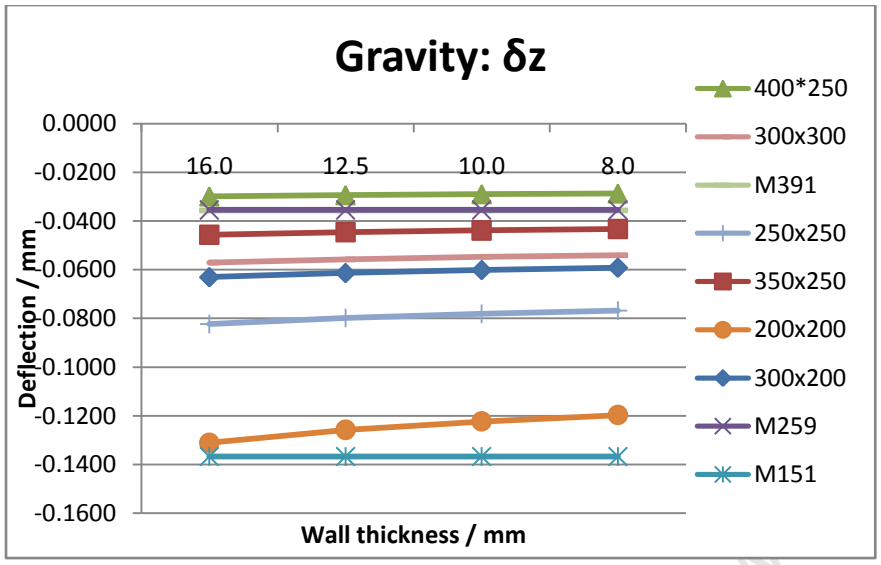

Figure 55: Axial deflection of horizontal gravity simulation.

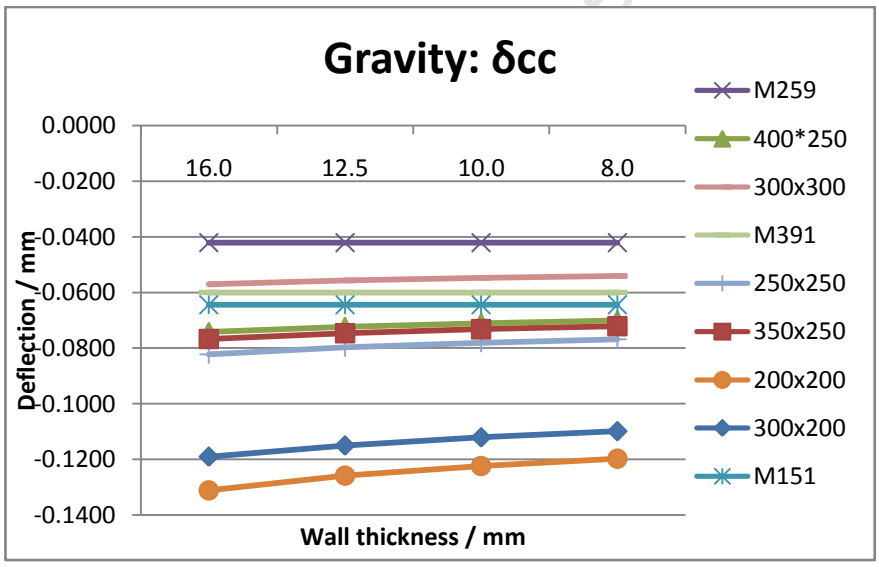

Figure 56: Circumferential deflection of vertical gravity simulation.

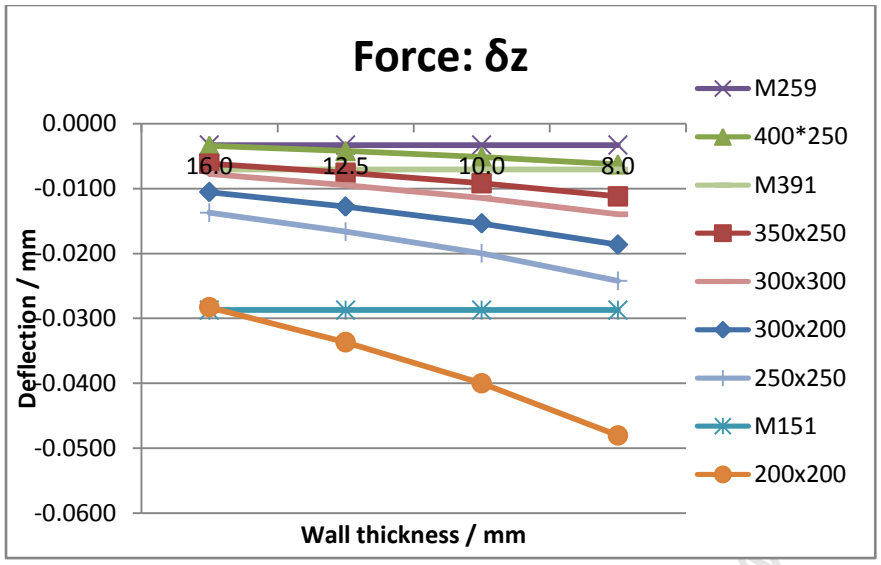

Figure 57: Axial deflection in force simulation.

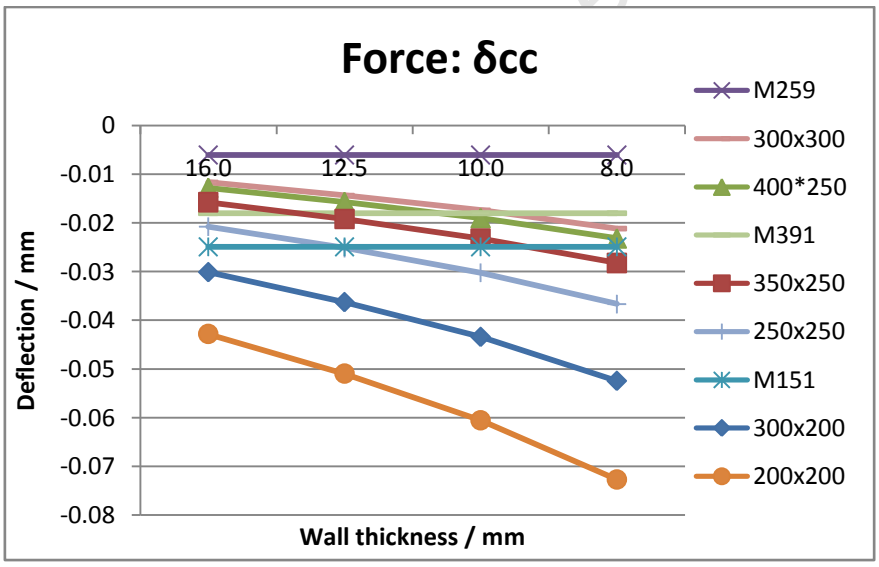

Figure 58: Circumferential deflection in force simulation.

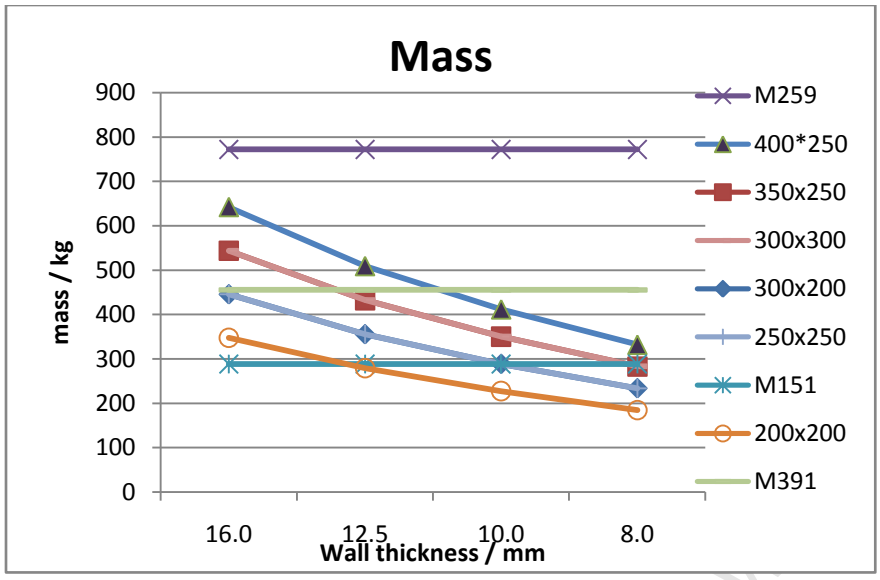

Figure 59: Comparison of section masses.

6. Validation

On completion of the M391 machine as per Figure 60, it was hereby necessary to validate the designs presented within this project. The main objective of the validation tests was to assess the performance and usability of the internal referencing system. This testing involved assessing the performance of the new feet used in the M391 machine as well as the referencing surfaces. The pitch and roll features were tested for functionality. The final assessment was that of the achievable un-flatness with the machine.

Figure 60: M391 circular milling machine.

6.1. Internal Referencing System Validation

6.1.1. Internal Referencing System Validation Process

The following process was used for validating the internal referencing system. The machine was mounted to the operating surface. All 8 feet were adjusted to have contact with the welding plate such that the two spherical mating surfaces were in full contact. Thereafter the welding plates were welded to secure them to the operating surface.

The next step was to retract 4 alternate adjustment screws so that that the machine was supported on the remaining adjustment screws. This forms a cross for the adjustment about two axes. Two feet positioned 180° to each other are first adjusted. The Z-axis height of the cassette assembly is measured when the arms are in an orientation so that the tool is aligned with each foot. From the values, the two are adjusted so that the height at both positions approach the mean of the original measurements. This process rotates the machine about the axis created by the two perpendicular feet.

The next step is to adjust the perpendicular feet. The same process was followed as with the first two positions by adjusting towards the mean of the chosen positions. At this point the two sets are level with respect to each other but may not be at the same height. In order to compensate for this two of the opposing positions are adjusted by the same amount in order to adjust their mean height to meet the orthogonal positions as required.

At this point the four secured points are within tolerance. In the tests performed the un-flatness between the four secured points was 0.01mm as illustrated by the upper points of the ‘before’ line in Figure 61. The lower points on the ‘before’ line correspond to the tool height at the unsupported points. In correlation with the previous predictions and findings the half supported profile follows an approximately sinusoidal path. It is worth noting that at this point the un-flatness reflected by the 8-point profile path is 0.16mm and is within tolerance according to the values used for the tests in section 4.3.1.

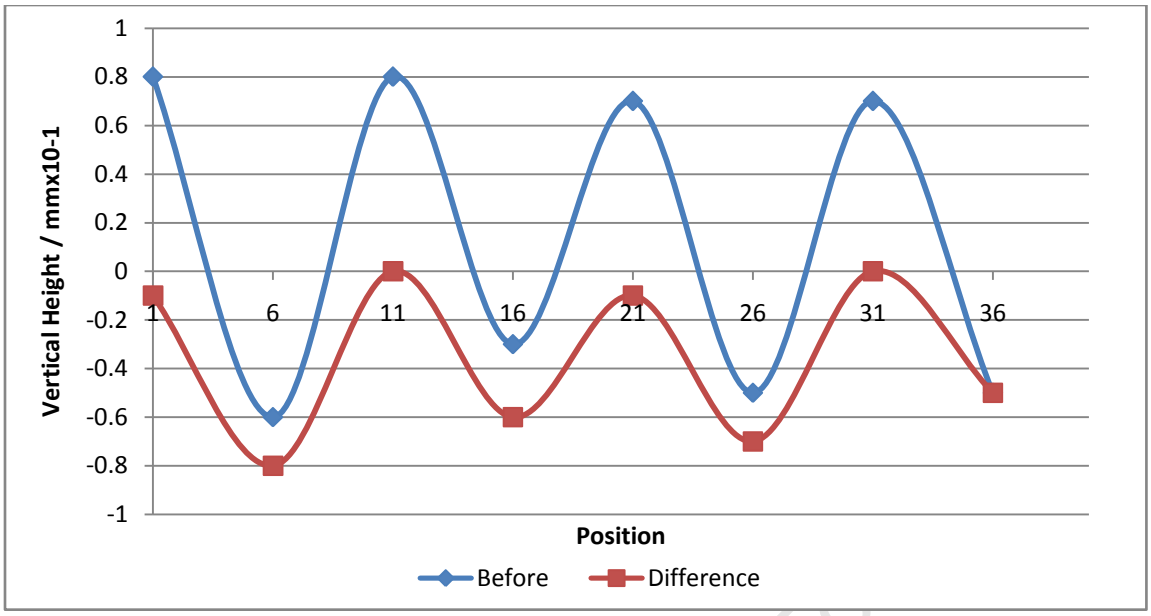

Figure 61: M391 setup with 4 legs secured.

The second phase of the internal referencing test was to attach a dial gauge to one of the arms or to the tool whereby possible and thus position this on one of the adjusted interfaces reference surface as illustrated in Figure 62. Herewith the gauge was set at 0.00mm. In Figure 61 the line labelled 'difference' represents the height reflected by the dial gauge at each of the eight reference surfaces. As reflected, the two lines show strong correlation where the unsupported feet and corresponding reference surfaces 'sag' in a similar manner to the tool.

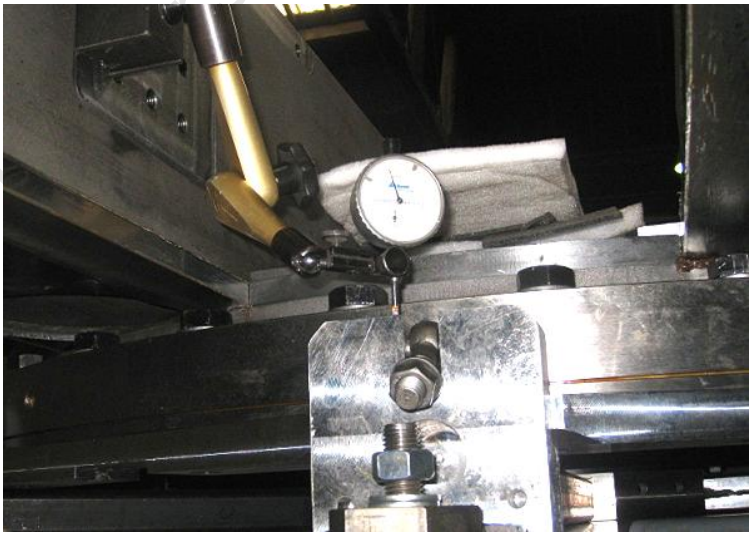

Figure 62: Dial gauge being used in with the internal reference.

The final stage is to adjust the unsupported legs to bring them into a load carrying state. This is achieved when the arms are positioned corresponding to the point of adjustment and the dial gauge measures the position of the reference surface. The foot is adjusted to reflect the same 0.00mm value attained from the pre set positions. This process ensures the bearing is resting on a flat, controlled surface.

Figure 63 below reflects the results of the setup using the internal referencing system. As illustrated, an overall un-flatness of **0.02mm** was attained at ϕ3500m. This result serves as validation of the function of the internal referencing system.

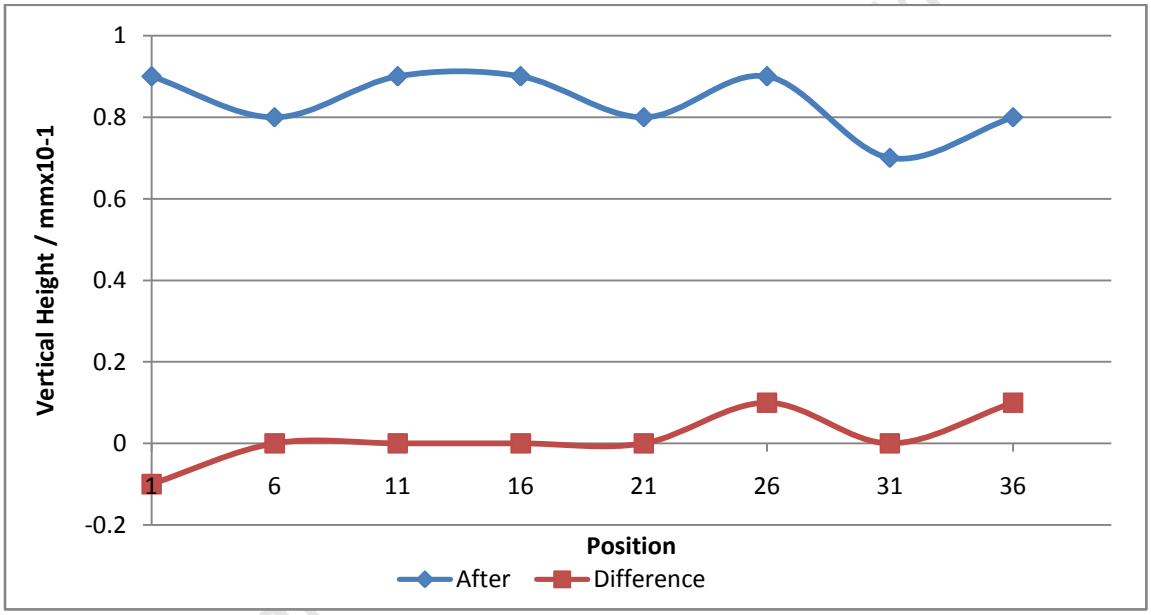

Figure 63: M391 setup with 8 legs secured using internal reference plane.

In this test a digital level was used for the initial setup with four legs. However, as discussed before, this is not always possible. In the event that these instruments are unusable, it is proposed that the user can follow the protocol laid out for the external referencing measurement with a dual gauge referencing to the surface with the initial 4 legs. This will attain a general orientation for the machine. This will then be followed by using the internal reference to ensure the required un-flatness is met.

6.1.2. M391 Feet

In the validation tests, the new design for the M391 feet illustrated in Figure 64 was assessed. When adjusting with the single point foot it was evident that there was little interference with the adjacent values. It is reasonable to expect a minor interference due to the induced deformation effecting the entire structure, although with the new feet the phenomenon was symmetric and predictable.

The use of the M45 x 1.5 threads allowed the adjustments to be performed with a resulting height change in 0.01mm increments. This fine resolution allowed the high accuracy setups to be attained with ease. When tightening the securing screw, the maximum change reflected on the arm was 0.01mm, an improvement from the previous designs.

Figure 64: M391 Foot.

6.2. M391 Achievable Un-Flatness

The final test with the M391 was to assess the machine to investigate the limit of accuracy. It was not possible to mill due to delivery time of the electro-mechanical systems of the machine being outside of the timeframe of this project. It was however possible to assess the unengaged profile of the M391 circular mill.

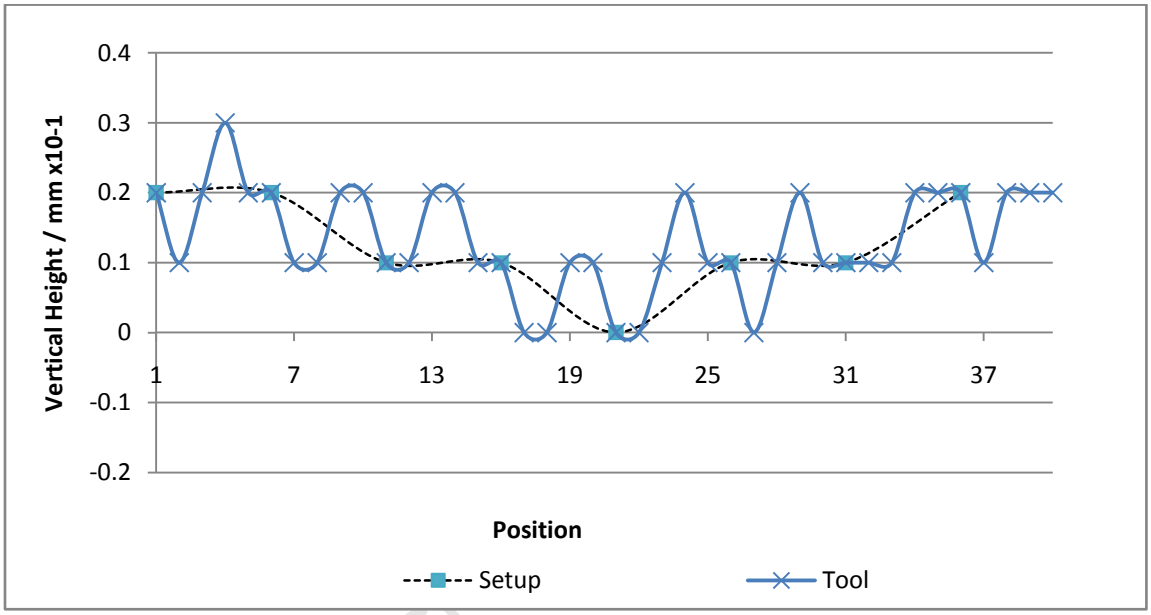

Figure 65: M391 test for limit to un-flatness.

The results from the investigation are given below in Figure 65. The points corresponding to the 8 points of adjustment were used for the setup. Here the setup points had an un-flatness of 0.02mm. From the results given it can be seen that the tool followed an oscillating pathway as experienced with both the M151 and M259.

Theoretical un-flatness	Φ3500mm
M391	**0.0138mm**

7. Conclusions

The objective of this project was to improve accuracy and repeatability in on-site circular milling through design of new systems. In order to achieve this it was necessary to analyse the current systems and the process of circular milling.

It was established that on-site circular milling does share certain functional aspects with regular in house milling, although the machine construction and design does differ greatly. This results in machine tools that are not only aesthetically dissimilar to regular machine tools but can function in a different manner.

The inherent nature of on-site machining signify that these machines are portable and are required to be assembled to be within tolerance at each individual work piece. This places a great reliance on the quality of the existing work piece references as well as the measuring equipment used.

It has been noted that the sensitive measuring equipment used for the alignment of on-site circular mills are subject to interference from a wide range of environmental factors that are often experienced when operating in the type of heavy industry that these machines are designed for. A factor that needed to be considered was that of availability of equipment, with these machine tools being contracted to work around the globe often in remote areas, availability or potential failure of the measurement equipment could rule out the use completely.

These factors have emphasised the need to incorporate systems into the machine tool design that would allow the same degree of accuracy to be attained repeatedly without having to rely on the sensitive measurement equipment that is not always available.

In order to create a system that allowed this functionality, it became necessary to test the circular mills operation and analyse the results of these tests. The results of these were used to isolate features that would allow the machine tool to operate at high levels of accuracy. These tests also provided an opportunity to investigate the sources of error in the process as well as environmental factors that would effect the performance of the measurement equipment.

It was proved in the tests of the existing machines that the main contributing factor to the outcome of the circular milling process was the alignment process and the steps taken to ensure that the machine tool operates within tolerance. In light of the measurement range applicable to this project there was a strong correlation between the paths traversed by the tool in unengaged activity to that of the engaged activity. This unengaged path was directly determined by the alignment process used.

The final alignment process was directly determined by the adjustment of the feet which brings the bottom base into which the bearing rests into alignment. It was suggested that by controlling the manufacturing process of the bottom base components, it would be possible to create reference surfaces that could be used to make the final un-flatness adjustments for the machine tool relative to itself. A system like this would eliminate the need for the use of sensitive measurement equipment in order to repeatedly attain high levels of accuracy in the form of low un-flatness values.

The secondary objective of the tests was to investigate the potential for a limit to the achievable level of performance in the circular milling process. The findings of which, emphasised that there was a limit to the achievable performance. ***This limit was a result of the machine tool design***. Here the smaller M151 displayed a **0.027mm** limit of un-flatness and the M259 a limit of **0.099mm**. The results were counterintuitive, given the larger seemingly sturdier construction of the M259 circular mill. However, this brought to light a subtle difference in the designs of the machines that was potentially the cause of the reduced performance.

Following on from the findings in the two tests, the new designs were produced to incorporate the features in facilitating improvement within the milling process. These systems included the internal referencing system, new foot design, pitch control, roll control and 8 leg bottom base. It was also proposed that the design requirement for using two arms to secure the milling tool assembly would facilitate the improvement of the performance of the M391 circular mill.

Once constructed, the M391 machine was assembled for validation. The validation of the internal referencing system was a success. The test yielded an 8 point setup un-flatness of **0.02mm** when the 4 point setup had an un-flatness of **0.01mm** prior to adjustment with the internal referencing system. During the validation process the function of the new foot design was found to be an improvement on previous designs. This in combination with the 8 leg system proved to be a more intuitive adjustment process.

The final stage of the validation was to assess the limit to the achievable un-flatness in the M391 machine. It was not possible to assess the performance with engaged activity as with the M151 and M259, although the unengaged orbit was assessed in the same manner. The result of this test was **0.0138mm**. This being a significant improvement in performance compared to that of the existing technologies.

From the results achieved, this project can be viewed as an overall success. A system was created that allows for results to be achieved that were previously unattainable in all circumstances. The functions of the supporting designs were found to behave in consistent manner and the overall achievable accuracy was improved.

By implementing improvements such as these found in this project, it enables designers that utilise these features to design to a higher degree of quality. This in turn can increase the bearing lifespan and reduce the frequency of downtime for maintenance due to poor mating surfaces causing raceway wear.

On-site machining is a scarcely researched subject. Continual and advanced research will inevitably benefit the industries that make use of on-site machining, as well as potentially opening up the possibilities to incorporate the technologies in currently unexplored areas.

8. References

[1]. World wind energy association WWEA. *World wind energy report 2009*. www.wwindea.org [2010, June 20].

[2]. Rothe Erde GmbH. www.rotheerde.de. [2010, May 28].

[3]. ITSUSA. *AX48-120.* http://www.ltsusa.com/db/tlfiles/AX48120%20Flange%20Facing%20Machine.pdf. [2010, July 29].

[4]. Climax Portable Machine Tools Inc. *CM6000*. http://www.cpmt.com/sites/default/files/CM6000%20Circular%20Mill.pdf. [2010, June 20]

[5]. Self Leveling Machines. *CSLM.* http://slm-onsite.com/machinery.html#cslm. [2010, June 25].

[6]. Fischer, Gomeringer, Heinzler, Kigus, Naher, Oesterle, Paetzold, Stephan. *Mechanical and metal trades handbook.* Haan-Gruiten - Europa Lehrmittel, 2006.

[7].Global bearing services. *General techinical information slewing bearings.* www.globalbearingservices.com/pdf/General%20Technical%20Information%20Slewing%20Bearings.pdf. [2009, August 15].

[8]. Rothe Erde GmbH. *Rothe Erde slewing bearing catalog.* www.rotheerde.com/download/info/Rothe_Erde_GWL_GB.pdf. [2009, July 18]

[9]. Stephenson, D. A., Agapiou, J.S. *Metal cutting theory and practice,* 2nd ed. CRC press, 2006. 447-468

[10]. Toropov, A. Ko, S. L., Prediction of shear angle for continuous orthogonal cutting using thermo-mechanical constants of work material and cutting conditions. *Journal of Materials Processing Technology,* Elsevier .182:167–173. (2007) 43-54

[11]. DeVries, W. R. *Analysis of material removal processes.* Springer texts in Mechanical Engineering, 1992.

[12]. Smith, G. T. *Industrial Metrology: surfaces and roundness.* Springer-Verlag London, 2002.

[13]. Davim, J. P. *Surface integrity in machining.* Springer, 2010. *51-52*

[14]. Menzel, M. 'The development of levels during the past 25 years, with special emphasis on the NI002 optical geodetic level and Dini 11 digital level.' *Carl Zeiss Jena GmbH.* www.ioes-co.com/src/contentfile/127.pdf. [2010, Jan 08].

[15]. Feist, W., Gürtler, K., Marhold, T., Rosenkranz, H. The new digital levels DiNi 10 and DiNi 20. *Vermessungswesen und Raumordnung,* Ferd. Dümmlers Verlag, 57(2): 65-76. (1995)

Appendix A: Milling Test Results

Appendix A contains the tabular results from the milling tests of the M151 and M259 circular milling machines in section 4.

	UF=1.2	UF=1.7	UF=0	max=0.2
Position	Setup	Tool	Surface	Tool-Surf
1		-0.4		
2		-0.3	-0.3	0
3	-0.1	-0.1	-0.1	0
4		0.1	-0.1	0.2
5		0.5	0.4	0.1
6		0.5	0.7	0.2
7		0.7	0.9	0.2
8		1	1	0
9	1.1	1.1	1.2	0.1
10		1.3	1.4	0.1
11		1.3	1.3	0
12		0.9	1.1	0.2
13		0.8		
14		0.8		
15	0.6	0.6		
16		0.6		
17		0.5		
18		0.5		
19		0.6		
20		0.7		
21	0.7	0.7		
22		0.9		
23		1		
24		1.2		
25		1.1		
26		1		
27	1	1		
28		0.8		
29		0.7		
30		0.6		
31		0.6		
32		0.5		
33	0.4	0.4		
34		0.1		
35		-0.2		
36		-0.4		

Table 14: In tolerance test results M151, Figure 40.

	UF=0.7	UF=1.6	UF=0	max=0.1
Position	Setup	Tool	Surface	Tool-Surf
1	-0.2	-0.2	-0.2	0
2		-0.1	0	0.1
3		-0.2	-0.3	0.1
4		-0.7	-0.7	0
5		-1.1	-1	0.1
6		-0.8	-0.7	0.1
7	-0.4	-0.4	-0.5	0.1
8		0.3	0.2	0.1
9		0.4	0.4	0
10		0.5		
11		0.3		
12		0.3		
13	0.2	0.2		
14		0.1		
15		0		
16		0.1		
17		-0.2		
18		-0.3		
19	-0.3	-0.3		
20		-0.1		
21		0		
22		0.1		
23		0		
24		0.1		
25	0.3	0.3		
26		0.4		
27		0.4		
28		0.2		
29		0.1		
30		0.1		
31	0	0		
32		-0.1		
33		-0.1		
34		-0.2		
35		-0.2		
36				

Table 15: In tolerance test results M259, Figure 41.

	UF=0.2	UF=0.4		max=0.1	UF=19
Position	Setup	Tool	Surface	Tool-Surf	3 legs
1		0			-9
2		0			
3	0.1	0.1			
4		0.2			
5		0.3	0.2	0.1	
6		0	0	0	
7		0.1	0.1	0	9.5
8		0.2	0.3	0.1	
9	0.3	0.3	0.4	0.1	
10		0.4	0.4	0	
11		0.3	0.2	0.1	
12		0.1	0.1	0	
13		0.1	0.1	0	-6.6
14		0.1	0.2	0.1	
15	0.2	0.2	0.2	0	
16		0.3			
17		0.3			
18		0.1			
19		0			10
20		0			
21	0.1	0.1			
22		0.2			
23		0.2			
24		0			
25		0.1			-8.6
26		0.1			
27	0.2	0.2			
28		0.3			
29		0.3			
30		0.2			
31		0.1			8.9
32		0.2			
33	0.2	0.2			
34		0.3			
35		0.3			
36		0.1			

Table 16: Un-flatness limit and three leg setup test results M151, Figure 38 and Figure 42.

	UF=0.2	UF=1.2		max=0.1	UF=24.7
Position	Setup	Tool	Surface	Tool-Surf	3 legs
1	0.3	0.3	0.2	0.1	14.2
2		0.4	0.4	0	
3		-0.2	-0.3	0.1	
4		-0.7	-0.6	0.1	
5		-0.4	-0.4	0	
6		0.2	0.3	0.1	-8.5
7	0.5	0.5	0.4	0.1	
8		-0.1	0	0.1	
9		-0.7	-0.6	0.1	
10		-0.7			
11		0.1			13.8
12		0.3			
13	0.4	0.4			
14		-0.3			
15		-0.7			
16		-0.5			
17		0.2			-7.2
18		0.4			
19	0.5	0.5			
20		0			
21		-0.5			
22		-0.5			
23		0.2			
24		0.4			15.1
25	0.3	0.3			
26		-0.2			
27		-0.5			
28		-0.2			
29		0.2			-8.4
30		0.4			
31	0.3	0.3			
32		-0.1			
33		-0.5			
34		0.1			16.2
35		0.3			
36					

Table 17: Un-flatness limit and 3 leg setup test results M259, Figure 39 and Figure 43.

	Tool	Surface	Uncertainty
1	0	0.1	0.1
2	-1.1	0.2	1.3
3	0.3	0.4	0.1
4	0.5	0.4	0.1
5	-0.5	-0.2	0.3
6	-0.5	0.5	1
7	-0.6	0.4	1
8	-1.8	0.7	2.5
9	-0.3	0	0.3
10	-0.5	0.9	1.4
11	1.3	1.2	0.1
12	0.9	1.2	0.3
13	0.8	1.1	0.3

Table 18: Vibration influence, Figure 45.

Appendix B: Results of 5.4.5. Simulation 2

Appendix B contains the tabular results of the arm profile simulations found in section 5.4.5.

				Gravity		Force	
				Horizontal	Vertical		
		kg	t / mm	δz / mm	δcc / mm	δz / mm	δcc / mm
DIN 10210	300x200x16mm	446	16.0	-0.0630	-0.1190	-0.0105	-0.0301
DIN 10210	300x200x12.5mm	356	12.5	-0.0613	-0.1150	-0.0128	-0.0362
DIN 10210	300x200x10mm	289	10.0	-0.0601	-0.1121	-0.0153	-0.0434
DIN 10210	300x200x8mm	234	8.0	-0.0591	-0.1099	-0.0186	-0.0525
DIN 10210	350x250x16mm	544	16.0	-0.0456	-0.0767	-0.0062	-0.01574
DIN 10210	350x250x12.5mm	433	12.5	-0.0445	-0.0746	-0.0076	-0.0192
DIN 10210	350x250x10mm	350	10.0	-0.0438	-0.0732	-0.0092	-0.02319
DIN 10210	350x250x8mm	283	8.0	-0.0433	-0.0721	-0.0112	-0.02822
DIN 10210	400x250x16mm	642	16.0	-0.0298	-0.0742	-0.0034	-0.01278
DIN 10210	400x250x12.5mm	509	12.5	-0.0293	-0.0723	-0.0042	-0.01566
DIN 10210	400x250x10mm	412	10.0	-0.0289	-0.0710	-0.0051	-0.01898
DIN 10210	400x250x8mm	332	8.0	-0.0286	-0.0700	-0.0062	-0.02315
DIN 10210	200x200x16mm	348	16.0	-0.1311	-0.1311	-0.02827	-0.04282
DIN 10210	200x200x12.5mm	279	12.5	-0.1258	-0.1258	-0.03365	-0.05097
DIN 10210	200x200x10mm	228	10.0	-0.1223	-0.1223	-0.03998	-0.06055
DIN 10210	200x200x8mm	185	8.0	-0.1197	-0.1197	-0.04801	-0.07271
DIN 10210	250x250x16mm	446	16.0	-0.08227	-0.08227	-0.01372	-0.02078
DIN 10210	250x250x12.5mm	356	12.5	-0.07975	-0.07975	-0.0166	-0.02515
DIN 10210	250x250x10mm	289	10.0	-0.07808	-0.07808	-0.01995	-0.03022
DIN 10210	250x250x8mm	234	8.0	-0.07679	-0.07679	-0.02418	-0.03663

DIN 10210	300x300x16mm	544	16.0	-0.05705	-0.05705	-0.00773	-0.01165
DIN 10210	300x300x12.5mm	433	12.5	-0.05569	-0.05569	-0.00946	-0.01433
DIN 10210	300x300x10mm	350	10.0	-0.05474	-0.05474	-0.01145	-0.01734
DIN 10210	300x300x8	283.2	8.0	-0.05403	-0.05403	-0.01396	-0.02114
Wagner	M259	772	-	-0.0354	-0.0421	-0.0033	-0.00604
Wagner	M151	288	-	-0.1367	-0.0644	-0.0287	-0.02489
Wagner	M391	455		-0.0356	-0.0600	-0.0071	-0.01799

Table 19: Results of Section 5.4.5 – simulation 2.

Appendix C: M391 Validation Results

Appendix D contains the tabular results from the validation tests of the M391 circular milling machine found in section 6.

	Before	Difference	After	Difference
1	0.8	-0.1	0.9	-0.1
6	-0.6	-0.8	0.8	0
11	0.8	0	0.9	0
16	-0.3	-0.6	0.9	0
21	0.7	-0.1	0.8	0
26	-0.5	-0.7	0.9	0.1
31	0.7	0	0.7	0
36	-0.5	-0.5	0.8	0.1

Table 20: Internal reference system validation results, Figure 61 and Figure 63.

	UF=0.2	UF=0.3	UF=1.5
Position	Setup	Tool	4 Legs
1	0.2	0.2	0.8
2		0.1	
3		0.2	
4		0.3	
5		0.2	
6	0.2	0.2	-0.7
7		0.1	
8		0.1	
9		0.2	
10		0.2	
11	0.1	0.1	0.8
12		0.1	
13		0.2	
14		0.2	
15		0.1	
16	0.1	0.1	-0.3
17		0	
18		0	
19		0.1	
20		0.1	
21	0	0	0.7
22		0	
23		0.1	
24		0.2	
25		0.1	
26	0.1	0.1	-0.5
27		0	
28		0.1	
29		0.2	
30		0.1	
31	0.1	0.1	0.5
32		0.1	
33		0.1	
34		0.2	
35		0.2	
36	0.2	0.2	-0.6
37		0.1	
38		0.2	
39		0.2	
40		0.2	

Table 21: Un-flatness test results M391, Figure 65.

Appendix D: Drawings

Appendix D contains the technical drawings for the designs found in section 5.